Active tectonics and late Cenozoic strain distribution in central and eastern Iran

Richard Walker and James Jackson

Bullard Laboratories, Department of Earth Sciences, University of Cambridge, Cambridge, UK

Received 31 March 2003; revised 20 April 2004; accepted 25 June 2004; published 7 October 2004.

[1] Right-lateral shear between central Iran and Afghanistan is accommodated on N–S right-lateral strike-slip faults surrounding the aseismic Dasht-e-Lut. North of ~34°N, the right-lateral shear is accommodated on left-lateral faults that rotate clockwise about vertical axes. Little is known of the late Tertiary and younger offsets and slip rates on the active fault systems, results that are important for understanding the regional tectonics. We use observations from satellite imagery to identify displaced geological and geomorphological markers, which we use in conjunction with the overall morphology and orientation of the active fault systems to estimate the total cumulative right-lateral shear. Estimates of cumulative fault movements from offset features and inferred vertical axis rotation of fault-bounded blocks suggest that the late Cenozoic strain is concentrated toward the eastern margin of Iran, along the Sistan shear zone, where bedrock offsets of at least 70 km are observed across the active faults. The geomorphology of the Deh Shir, Anar, and Great Kavir strike-slip faults in central Iran suggest that although little shortening is accommodated across this region, they might still be active, and hence capable of producing earthquakes. Present-day activity on these faults in central Iran would not be expected from distributions of instrumental and historical earthquakes. Although speculative, the late Tertiary strain distribution described in this paper is consistent with what we know of the present-day rates of shear in eastern Iran and provides a framework to which later, more detailed, work can be added. *INDEX TERMS:* 8107 Tectonophysics: Continental neotectonics; 8102 Tectonophysics: Continental contractional orogenic belts; 1208 Geodesy and Gravity: Crustal movements—intraplate (8110); 8040 Structural Geology: Remote sensing; 9320 Information Related to Geographic Region: Asia; *KEYWORDS:* active tectonics, Iran, strike-slip faults. **Citation:** Walker, R., and J. Jackson (2004), Active tectonics and late Cenozoic strain distribution in central and eastern Iran, *Tectonics*, *23*, TC5010, doi:10.1029/2003TC001529.

0278-7407/04/2003TC001529

1. Introduction

[2] In this paper, we investigate the late Cenozoic and recent deformation in central and eastern Iran. In contrast to other parts of the Alpine-Himalayan system, in which active deformation is spread across regions several thousand kilometers wide [e.g., *Molnar and Tapponnier*, 1975], nearly all the convergence is accommodated in a relatively small area defined by the political borders of Iran, and provides a compact region for the study of continental collision (Figure 1).

[3] The general features of the present-day tectonics in this arid, sparsely populated region are broadly understood [e.g., *Berberian*, 1976, 1981; *Berberian and Yeats*, 1999; *Jackson and McKenzie*, 1984; *Nowroozi and Mohajer-Ashjai*, 1985; *Jackson et al.*, 1995], with major active oblique strike-slip and thrust faults observed in several clearly defined zones. However, little is known of the late Tertiary and younger offsets and slip rates on these active fault systems, results that are important for estimating potential seismic hazard in the region, and also for understanding the regional tectonics.

[4] In the first part of this paper, we use the distribution of historical and instrumental seismicity, a review of previously published work and indications of recent fault movements observed using Landsat thematic mapper plus (TM+) satellite imagery to infer the present-day distribution of active faulting in eastern Iran. Displaced geological and geomorphological markers, as well as the overall morphology and orientation of the major fault systems, are then used to estimate the total cumulative late Cenozoic displacements across the fault zones.

[5] We then combine all the available information into a self-consistent, though speculative, kinematic model of deformation in eastern Iran. Our approach relies on the assumption that little of the cumulative strain on the active faults is inherited from earlier tectonic episodes. Because of the lack of published information on the region we have little independent constraints on whether this is justified. However, the summed right-lateral displacement measured across the active faults agrees remarkably well with the total amount of right-lateral strain expected between central Iran and Afghanistan (as outlined in section 2). We do not know whether the distribution of cumulative late Cenozoic strain is representative of the present-day distribution of strain, as the slip rate across individual faults may have changed through time. However, in absence of any indications to the contrary, we use the cumulative strain distribution to assign tentative present-day slip rates to the active fault zones.

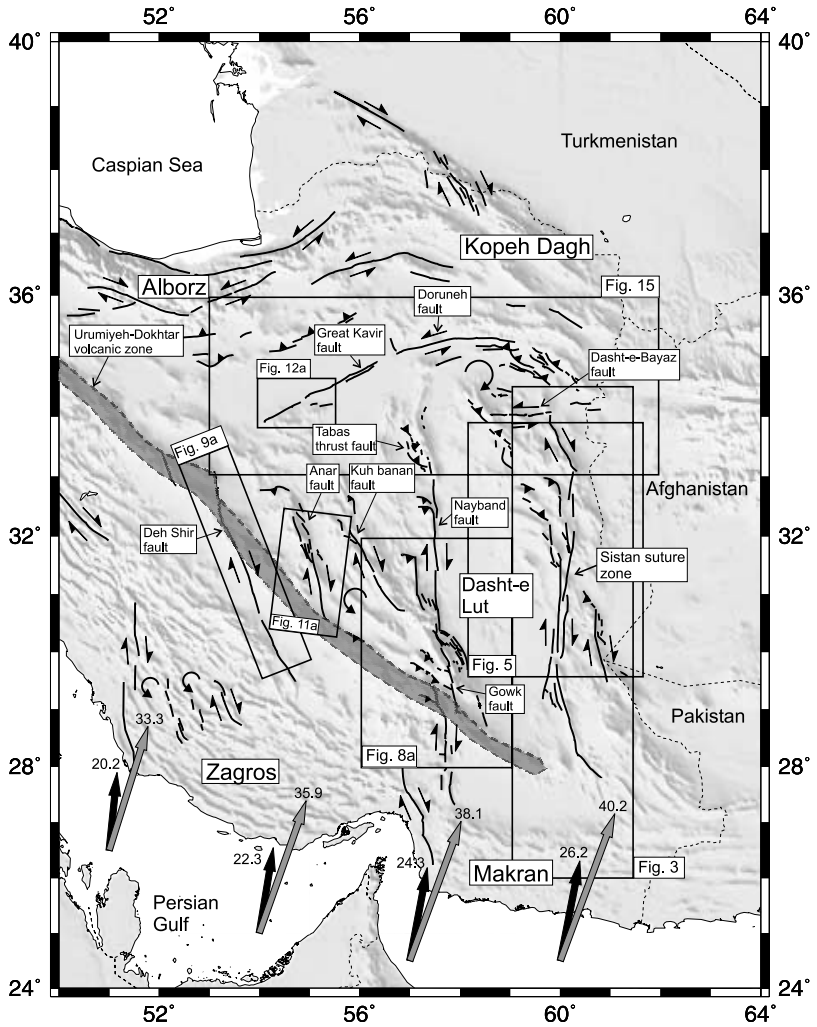

Figure 1. GTOPO30 image of central and eastern Iran showing the major fault zones and geographical regions. Black and gray arrows represent Arabia-Eurasia plate motions. Rates are in millimeters per year. Black arrows are GPS estimates from *Sella et al.* [2002] and gray arrows represent 3 Ma magnetic anomaly plate motions which are a combination of the Africa-Eurasia plate motion from *Chu and Gordon* [1998] and the Africa-Arabia plate motion of *DeMets et al.* [1994] (see *Jackson et al.* [1995] for method). Arabia-Eurasia convergence occurs in the Zagros, the Alborz, and Kopeh Dagh, and possibly in central Iran by the rotation of strike-slip faults (see later discussion). Right-lateral shear between central Iran and Afghanistan is taken up on N–S right-lateral faults of the Gowk-Nayband and Sistan suture zone systems, which surround the Dasht-e-Lut. North of 34°N, the right-lateral shear is taken up on left-lateral faults that rotate clockwise. Boxes show the regions covered by Figures 3, 5a–5c, 8a, 9a, 11a, 12a, and 15.

[6] Finally, we ask whether the record of seismicity (both instrumental and historical) is sufficient to delineate all of the actively deforming fault zones, particularly in central Iran, where GPS measurements show that little present-day shortening is accommodated [e.g., *Vernant et al.*, 2004], and where very few earthquakes are known to have occurred, and yet pristine fault scarps are preserved in the alluvial cover.

2. Active Tectonics

[7] The active deformation in Iran is caused by Arabia-Eurasia convergence. Nearly all of the shortening is accommodated within the political borders of Iran itself (Figures 1 and 2). Older global plate models that used a combination of Africa-Eurasia and Arabia-Africa motions to estimate the overall Arabia-Eurasia convergence show approximately N–S shortening in eastern Iran, with rates of about 30 mm/yr at 50°E and 40 mm/yr at 60°E [*Jackson*, 1992; *DeMets et al.*, 1994; *Jestin et al.*, 1994; *Chu and Gordon*, 1998]. More recent global models, constrained by GPS, suggest that these earlier estimates are too high, with only ~26 mm/yr of shortening at 60°E [*Sella et al.*, 2002]. Results from a regional GPS network again suggest that the total convergence across Iran is ~25 mm/yr in eastern Iran [*Vernant et al.*, 2004].

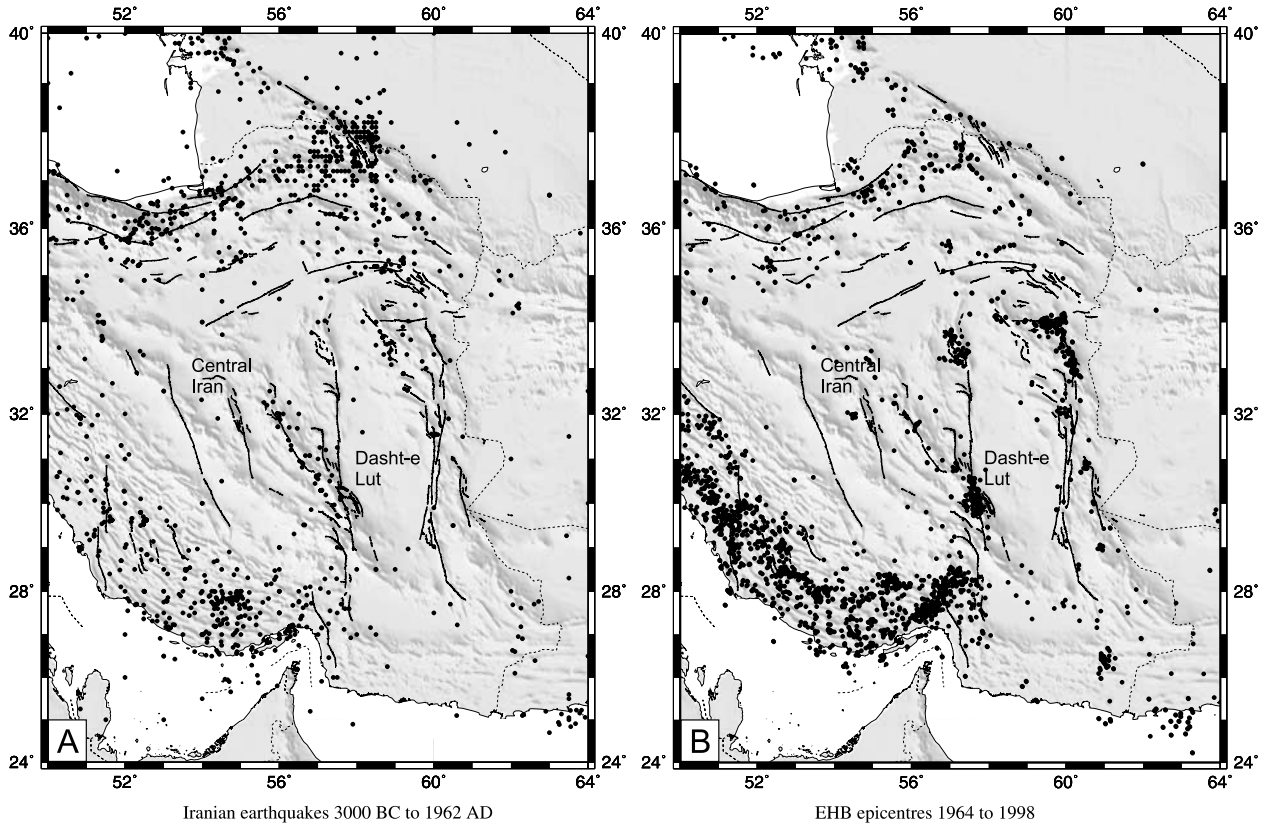

Figure 2. (a) Distribution of earthquake epicenters from historical records (3000 B.C. to 1962 A.D.) courtesy of N. N. Ambraseys [*Ambraseys and Melville*, 1982]. Seismicity is broadly confined to the Zagros, Alborz, and Kopeh Dagh mountain belts and to narrow N–S zones surrounding the Dasht-e-Lut. (b) Distribution of instrumentally recorded earthquake epicenters (1964 to 1998) from the catalogue of *Engdahl et al.* [1998]. The distribution is similar to that in Figure 2a, with seismicity confined to mountainous regions, and with very few epicenters in central Iran and the Dasht-e-Lut.

[8] Arabia-Eurasia convergence is accommodated in the Zagros mountains of SW Iran, and in the seismic belts of the central Caspian, the Alborz, and the Kopeh Dagh of northern Iran [e.g., *Vernant et al.*, 2004] (Figures 1 and 2). These deforming regions are separated by relatively aseismic desert depressions. Whatever shortening is not taken up in the Zagros must be expressed as N–S right-lateral shear between central Iran and western Afghanistan (Figure 1). This shear is accommodated on several major N–S right-lateral fault systems on both the west (Kerman province) and east (the East Iranian Ranges of Sistan province) sides of the Dasht-e-Lut, which is a flat, low-lying and aseismic block (Figure 2). North of 34°N, deformation is accommodated on left-lateral strike-slip faults that must rotate clockwise if they are to take up N–S right-lateral shear (Figure 1) [e.g., *Jackson and McKenzie*, 1984; *Walker et al.*, 2004].

[9] *Jackson and McKenzie* [1984, 1988] and *Jackson et al.* [1995] suggest that the Zagros accommodates about 10–15 mm/yr of present-day shortening. This estimate is very dependent on the assumptions they made, but is roughly compatible with local GPS studies indicating that the central Zagros accommodates ~10–12 mm/yr of shortening, which is approximately half of the total Arabia-Eurasia shortening at this longitude [*Tatar et al.*, 2002; *Hessami*, 2002]. If the eastern Zagros mountains at longitude 56°E accommodate roughly half of the ~26 mm/yr of shortening estimated from GPS-derived plate motions, which is the same proportion of the total Arabia-Eurasia convergence accommodated in the central Zagros [*Tatar et al.*, 2002; *Hessami*, 2002], then approximately 13 mm/yr of shortening must be taken up north of the Zagros, causing an equal amount of N–S right-lateral shear in eastern Iran. These arguments are supported by the results of a country-wide Iranian GPS network, which indicate ~15 mm/yr of right-lateral shear between central Iran and the Afghan border [*Vernant et al.*, 2004].

[10] Although central and eastern Iran are composed of various tectonic blocks, once separated by minor ocean basins [*Berberian and King*, 1981] that started to close in the Cretaceous [*McCall*, 1996], much of the broader collision zone did not start to deform until the mid-Miocene or even later [*Dewey et al.*, 1986]. In addition, a major reorganization of deformation appears to have occurred in many parts of the Arabia-Eurasia collision zone between 3 and 7 Ma (see *Allen et al.* [2004] for a full review). For

example, the possible onset of strike-slip faulting in western parts of the collision is dated at ~5 Ma [e.g., *Westaway*, 1994], a major reorganization is seen in the sedimentation and deformation in both the Alborz and South Caspian basin at ~6 Ma [e.g., *Devlin et al.*, 1999; *Axen et al.*, 2001; *Jackson et al.*, 2001; *Allen et al.*, 2002] and at ~5 Ma in the Kopeh Dagh [*Lyberis and Manby*, 1999]. Also, although the onset of folding along the Zagros is both poorly constrained and likely to be diachronous, previous work has suggested the onset of widespread folding across much of the belt may be as late as the Pliocene [*Falcon*, 1974; *Hessami*, 2002]. Although the reasons for this reorganization of the Arabia-Eurasia collision are not known, from the best age estimates it is likely to have occurred between 3 and 7 Ma across much of the region, and we expect that the present-day configuration of active faulting in eastern Iran dates from roughly this time [e.g., *Allen et al.*, 2004]. As shortening in the Kopeh Dagh is fed by right-lateral shear between central Iran and Afghanistan, we believe that the N–S right-lateral strike-slip faults in eastern Iran probably date from a similar time as the onset of deformation in the Kopeh Dagh at 5 Ma [*Lyberis and Manby*, 1999]. This reasoning implies that at the present-day rate of ~15 mm/yr of right-lateral shear between central Iran and Afghanistan, a total of ~75 km of right-lateral slip will have occurred on the faults east and west of the Dasht-e-Lut over the last 5 Ma, and up to 105 km if the faults have been active since 7 Myr ago. Although we cannot be sure that the rates of right-lateral shear in eastern Iran have been constant since 5–7 Ma, plate tectonic reconstructions indicate that the overall convergence has been uniform since ~56 Ma [*McQuarrie et al.*, 2003].

3. Seismicity

[11] The distributions of historical and instrumental seismicity are shown in Figure 2. Both show a broadly similar pattern, with concentrations of epicenters in the Zagros mountains in the south, and in the Alborz and Kopeh Dagh of northern Iran. Two roughly north-south seismic belts are also defined in eastern Iran. The confinement of seismic activity to regions of elevated topography, and the apparent absence of earthquakes within the arid depressions of central and eastern Iran, suggest that the distribution of seismicity delineates most of the actively deforming belts of Iran [e.g., *Jackson et al.*, 1995; *Ambraseys and Jackson*, 1998]. However, the instrumental earthquake record is almost certainly too short to reveal all the major individual faults, which may have earthquake repeat times of more than 1000 years [e.g., *Berberian and Yeats*, 1999]. Also, the historical record, although excellent, is unlikely to be complete, with a bias toward earthquakes that have damaged major population centers [*Ambraseys and Melville*, 1982]. Therefore, although few historical earthquakes are recorded from the deserts of central and eastern Iran (Figure 2), this could, to some extent, reflect the low population density of these arid, desert regions.

[12] However, we are confident that the lack of both historical and instrumental seismicity within central Iran and the Lut desert does, in the most part, reflect a lack of active deformation, which is supported by an absence of youthful tectonic landforms and fault scarps (although there are exceptions that we return to later; see section 4.3). Similarly, the relatively high levels of seismicity within surrounding mountain belts indicate that these are zones of active faulting and deformation. The majority of the large earthquakes can be associated with Holocene scarps and neotectonic features within these regions (section 4).

4. Distribution of Late Cenozoic Strain in Eastern and Central Iran

[13] The following section describes the cumulative late Cenozoic strain distribution in eastern Iran. The major fault systems around the Dasht-e-Lut region are oriented N–S, and are known to be right-lateral strike-slip faults from seismological and field investigations of earthquakes [e.g., *Berberian and Yeats*, 1999; *Berberian et al.*, 1999, 2001], from the right-lateral displacement of geomorphological features and rivers [e.g., *Tirrul et al.*, 1983; *Wellman*, 1966], and from the role of the faults in accommodating right-lateral shear between Iran and Afghanistan [e.g., *Jackson and McKenzie*, 1984]. For each fault system, we describe the available geological, geomorphological, and seismological data that characterize the nature of the faults. We then assess the total cumulative offsets of the various fault systems using our own observations and the results of previously published work. Although we confine ourselves to a description of the faulting, we use the results to develop a speculative kinematic model of late Cenozoic deformation in section 5. A proportion of the cumulative strain measured across the major faults may be inherited from earlier phases of deformation, which has implications for our model, as the strain distribution will not be wholly representative of the late Cenozoic. We are, however, confident that our estimates of total strain are representative of the most recent period of deformation, as they are supported by geomorphological reconstructions (in the case of the Gowk fault, see section 4.2) [*Walker and Jackson*, 2002], and by available structural data, which suggest that throughgoing north-south right-lateral faults of the Sistan suture zone are only seen in the most recent phase of deformation (section 4.1)[*Freund*, 1970].

4.1. Active Faulting in the Sistan Suture Zone: Eastern Dasht-e-Lut Margin

[14] A zone of north-south active right-lateral strike-slip faulting occurs along the eastern margin of the Dasht-e-Lut in the East Iranian mountain ranges, which roughly define the eastern border of Iran (Figure 3). The rocks within the East Iranian ranges define the Sistan suture zone (Figure 4) [*Tirrul et al.*, 1983]. This deformed accretionary prism was emplaced during the destruction in Late Cretaceous (Senonian)-Palaeocene times (~89 to 55 Myr ago) of a narrow arm of the Neo-Tethys ocean separating the structurally coherent Lut and Afghan continental blocks. The Sistan suture zone is composed of two accretionary prisms (the Neh and Ratuk complexes) separated by sediments and volcanics of the Sefidabeh forearc basin (Figure 4a) [*Tirrul*

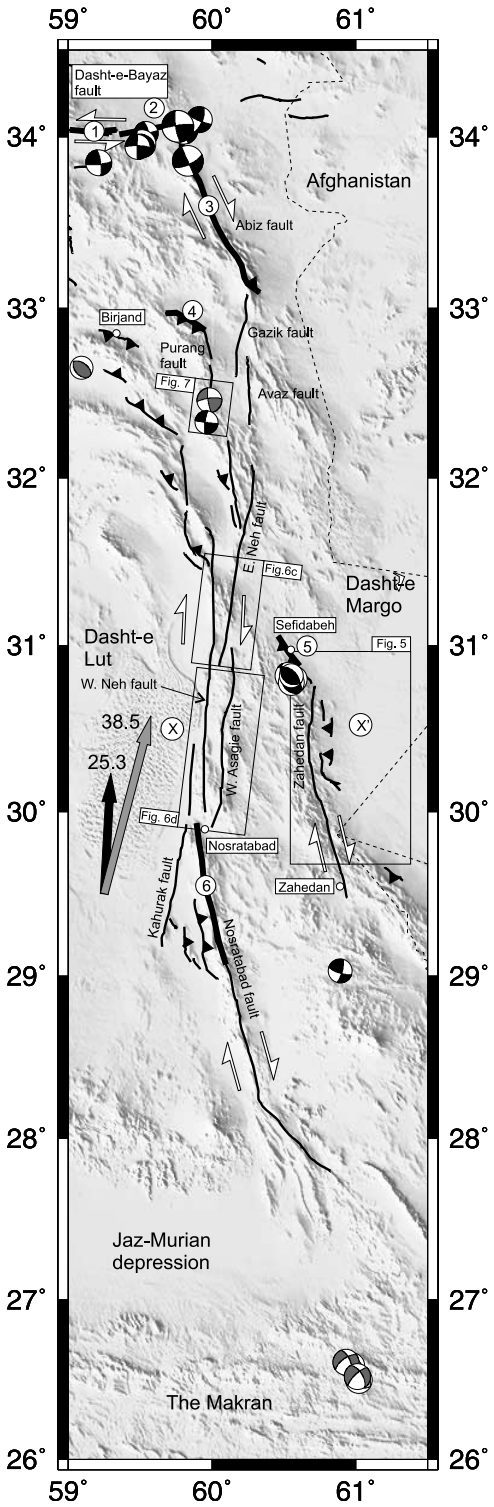

et al., 1983]. The Neh and Ratuk complexes are identifiably separate structural units, the former dating from Late Cretaceous (Senonian) to Eocene (~89 to 34 Ma), and the latter from the pre-Maastrichtian Cretaceous (>71 Ma), with different overall compositions and structural histories [*Tirrul et al.*, 1983]. The rock units dip steeply, and strike NW–SE. There have been three phases of deformation [*Camp and Griffis*, 1982; *Tirrul et al.*, 1983]. The earliest folding event produced E–W trending structures, which were subsequently refolded along NNW trending axial surfaces and dissected by conjugate left- and right-lateral strike-slip faults. These two deformation episodes occurred between the late Eocene and early Miocene. The third, ongoing, deformation event involves N–S right-lateral strike-slip faulting and associated folding and is probably related to the final closure of Arabia and Eurasia [e.g., *Berberian and King*, 1981]. The active right-lateral strike-slip faults cut through and displace units of the Sistan suture zone. Although the active faults may in part be inherited from earlier phases of deformation [e.g., *Berberian et al.*, 2000], the cumulative displacements across inactive early Tertiary faults are typically less than 1 km [*Freund*, 1970], unlike the >10 km displacements observed across active right-lateral faults. Therefore we are confident that restoration of displaced rock units across the active right-lateral faults will give some idea of the total Plio-Quaternary cumulative slip across the faults.

[15] The East Iranian ranges separate the arid desert depressions of the Dasht-e-Margo and Dasht-e-Lut (Figure 3). The active faults trend N–S to NNE–SSW in the central, narrow part of the ranges near latitude 34°N (Figure 3). Northward, several of the faults acquire a more NW–SE trend and end in thrust faults. Southward, the faults merge with active thrust faults of the Makran accre-

Figure 3. GTOPO30 topography of the East Iranian Ranges in Sistan province (see Figure 1 for location). Active strike-slip and thrust faults are marked as thin black lines. Black and gray arrows represent Arabia-Eurasia plate motions as in Figure 1. Fault plane solutions of shallow (<35 km) earthquakes are shown. Black solutions are events modeled using body waveforms (listed by *Jackson* [2001] and *Walker et al.* [2004]); dark gray represents events from the Harvard centroid moment tensor (CMT) catalogue with >70% double-couple component. Earthquake ruptures from some major earthquakes are shown as thickened lines. Circled numbers mark location of the following: 1, the 31 August 1968 Dasht-e-Bayaz earthquake [e.g., *Ambraseys and Tchalenko*, 1969]; 2, the 27 November 1979 Khuli-Buniabad earthquake [*Haghipour and Amidi*, 1980]; 3, the 10 May 1997 Zirkuh earthquake [*Berberian et al.*, 1999]; 4, the 1493 Nauzad earthquake [*Ambraseys and Melville*, 1982]; 5, the February 1994 Sefidabeh earthquake sequence (note that the ruptures developed during the Sefidabeh events consisted of secondary normal faulting above a blind thrust fault) [*Berberian et al.*, 2000]; 6, the 1838 Nosratabad earthquake [*Ambraseys and Melville*, 1982]. The line X–X′ is referred to in the text. Boxes mark the regions covered by Figures 5a–5c, 6c, 6d, and 7.

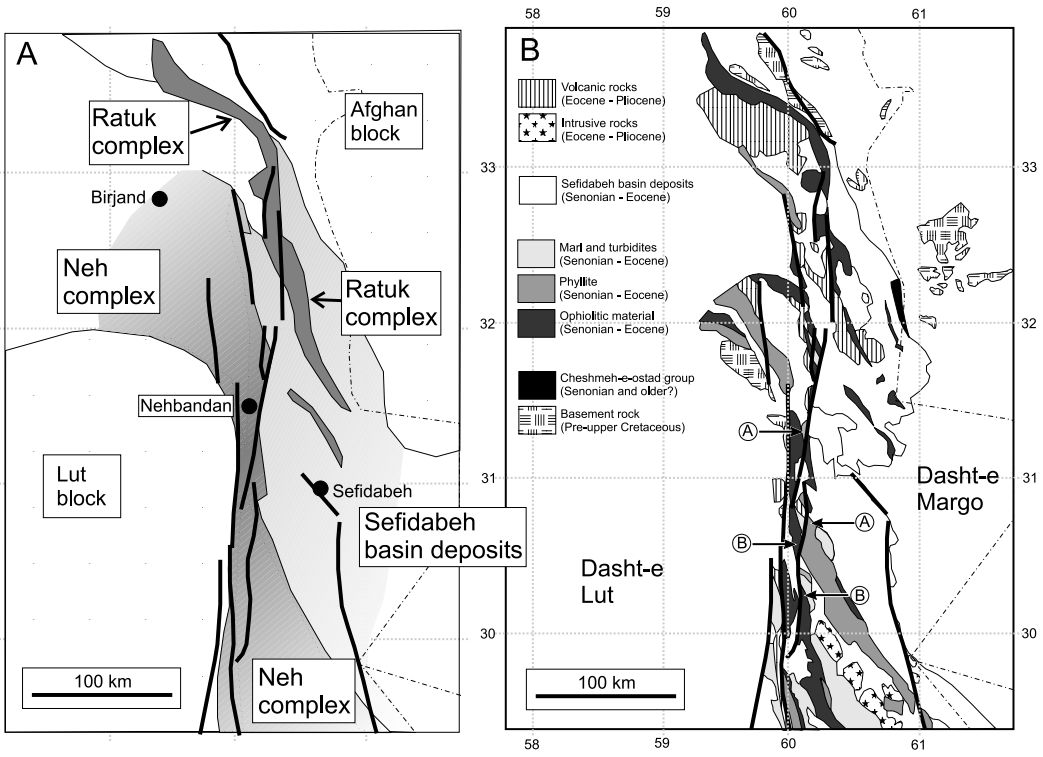

Figure 4. Geology of the Sistan suture zone (redrawn from *Tirrul et al.* [1983]). (a) Broad subdivisions of the Sistan suture zone. Two NW–SE trending deformed accretionary prisms (the Neh and Ratuk complexes) are separated by forearc deposits of the Sefidabeh basin. Active right-lateral strike-slip faults cut through and displace these units. (b) Subdivisions of the Sistan suture zone. Individual units of the Neh complex can be correlated across the active strike-slip faults, giving a displacement of ~50 km across the East Neh (West Asagie) fault (between points marked B; see section 4.1.2). *Tirrul et al.* [1983] obtain a maximum overall displacement of the Neh complex across the East Neh and West Asagie faults of ~65 km (between points marked A).

tionary wedge (Figure 3). In the central part of the Sistan ranges, cumulative fault scarps along the mountain flanks show a vertical component of motion, with scarps facing outward from the high ground, indicating that the east Iranian ranges are being uplifted with respect to both the Dasht-e-Lut and Dasht-e-Margo deserts. From the orientation of the faults with respect to the Arabia-Eurasia convergence vectors (e.g., Figure 3), the uplift probably reflects a slight shortening component across the fault zone.

[16] A major difference between the Sistan faults and their counterparts to the west of the Dasht-e-Lut (see section 4.2) is that several parallel fault strands appear to be active simultaneously across a very narrow zone. This configuration may result from an evolution in the pattern of faulting with time. However, three major right-lateral faults are seen at latitude 30.5°N (across line X–X′ in Figure 3; see also Figures 5a–5c and 6a–6d). The apparently youthful landforms associated with each of these faults, and a number of instrumental and historical earthquakes (e.g., Figure 3), suggests that they are active at the present day.

4.1.1. Zahedan Fault

[17] The Zahedan fault is the easternmost of the active faults and is ~150 km long (Figures 3 and 5a). Oblique motion across the fault zone appears to be spatially separated into strike-slip and thrust components. Movement on the Zahedan fault itself appears to be almost pure strike-slip [*Freund*, 1970; *Berberian et al.*, 2000], but numerous north-south folds expressed as low hills in alluvium east of the Zahedan fault accommodate some shortening (Figure 5b). At its northern end, the Zahedan fault ends at Palang Kuh in the Sefidabeh blind thrust that ruptured in a series of earthquakes in 1994 (Figures 3 and 5b) [*Berberian et al.*, 2000]. *Freund* [1970] used offset lithologies at the northern end of the fault to show ~13 km of total right-lateral offset on the fault (Figure 5b). Our observations support this, with offsets of at least 13 km, and possibly up to 20 km, in a Late Cretaceous to Eocene sequence of mudstones and phyllite in the mountains directly north of Zahedan (Figure 5c) [*Behruzi*, 1995].

4.1.2. Neh Faults

[18] The East and West Neh faults are two subparallel faults, 10 to 20 km apart. Although segmented, they both have a total length of ~200 km. To the south they end near Nosratabad (Figure 3). The Neh faults appear to link southward with the Kahurak and Nosratabad faults. To the north, the Neh faults enter a zone of several strike-slip and thrust faults that includes the Birjand, Purang, Gazik, and

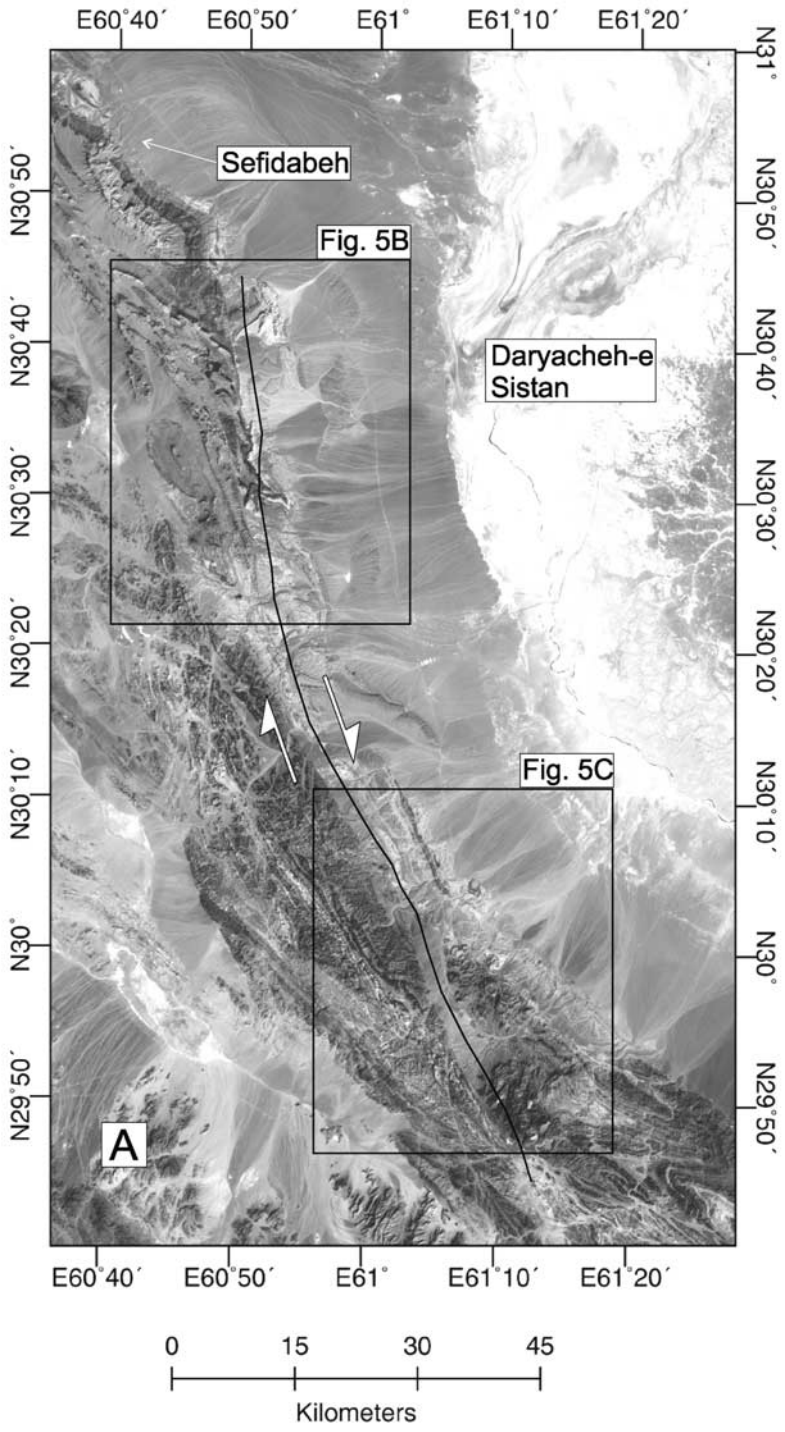

Figure 5. Landsat TM+ images of the Zahedan fault (see Figure 3 for location). (a) Overview of the entire fault; boxes show the extents of Figures 5b and 5c. (b) Close-up of the northern end of the fault. The fault ends at Palang Kuh, and links to the Sefidabeh blind thrust. Lithological units are displaced by ~13 km (points marked X and Y)[*Freund*, 1970]. Shortening across the fault zone is apparently accommodated on thrusts east of the strike-slip trace (folds in alluvium marked by black arrows). (c) Close-up of the southern end of the Zahedan fault near Zahedan. Late Cretaceous to Eocene mudstones and Phyllites are displaced by at least 13 km across the fault (points marked Z).

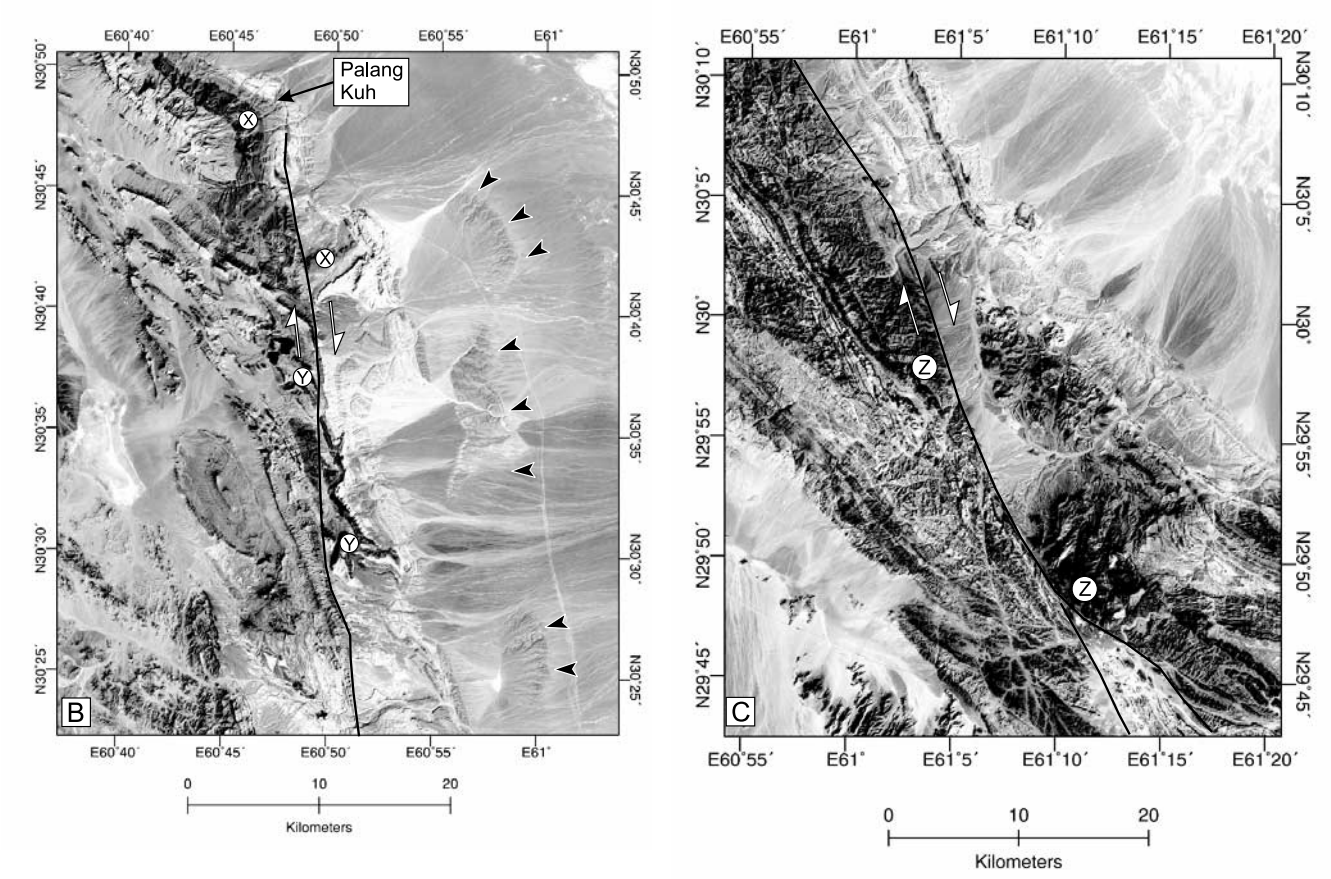

Figure 5. (continued)

Avaz fault systems (Figure 3). The Gazik and Avaz faults link in the north to the Abiz fault, parts of which have ruptured in twentieth century earthquakes, including the M_w7.2 10 May 1997 Zirkuh earthquake [*Berberian et al.*, 1999]. At its northern end, the Abiz fault links in turn with the left-lateral Dasht-e-Bayaz fault (Figure 3).

[19] The East Neh fault has two main segments, each ~100 km long, the southern of which is sometimes called the West Asagie fault (Figure 3) [*Aghanabati*, 1991]. Right-lateral drainage offsets are seen across the East Neh fault. Figure 6c shows a river offset at Khunik, where the Birjand-Zahedan road follows an offset river channel for ~5 km. The East Neh–West Asagie segment boundary occurs south of Khunik at latitude ~31°N. A direct connection between the East Neh and West Asagie fault segments is difficult to demonstrate, although they overlap for at least 20 km, and there is probably considerable active deformation within the bedrock mountains in this region.

[20] A distinctive ophiolitic sequence of Late Cretaceous peridotite and Tertiary turbidites and phyllites of the Neh complex are displaced across the southern (West Asagie) segment by at least 50 km (Figure 6a) [*Saidi*, 1989; *Eftekhar-Nezhad*, 1991]. *Tirrul et al.* [1983] suggest that the fault offset might be as much as 65 km, on the basis of an apparent offset of the entire Neh complex (Figures 4a and 4b).

[21] The West Neh fault is the westernmost of the Sistan faults, and shows a clear trace through young alluvium, with west facing scarps through which meandering rivers have incised (Figure 6d). Toward its northern end it displaces an assemblage of Jurassic phyllites and thin slivers of Cretaceous ophiolitic material [*Eftekhar-Nezhad*, 1990]. These displaced assemblages are shown in Figure 6b. The cumulative displacement of these rocks is difficult to quantify exactly, as the strike of the lithologies is at only a small angle from the strike of the West Neh fault, but is approximately 10 km.

4.1.3. Total Late Cenozoic Strain in the Sistan Suture Zone

[22] At the latitude of the line X–X′ in Figure 3, the Zahedan, East Neh (West Asagie) and West Neh faults are the only structures that show youthful cumulative scarps and displace young alluvium and river systems, and hence the major part of the late Cenozoic strain in the Sistan suture zone might be expected to be localized across them. The combined bedrock offset across these three faults, and hence across the whole Sistan fault system at latitude ~30.5°N, is at least 70 km, and possibly up to 95 km (13 to 20 km on the Zahedan fault, 50 to 65 km on the East Neh fault, and ~10 km on the West Neh fault). It is difficult to demonstrate similar fault offsets in the northern and southern parts of the fault system, as the faulting occurs on several shorter segments, and

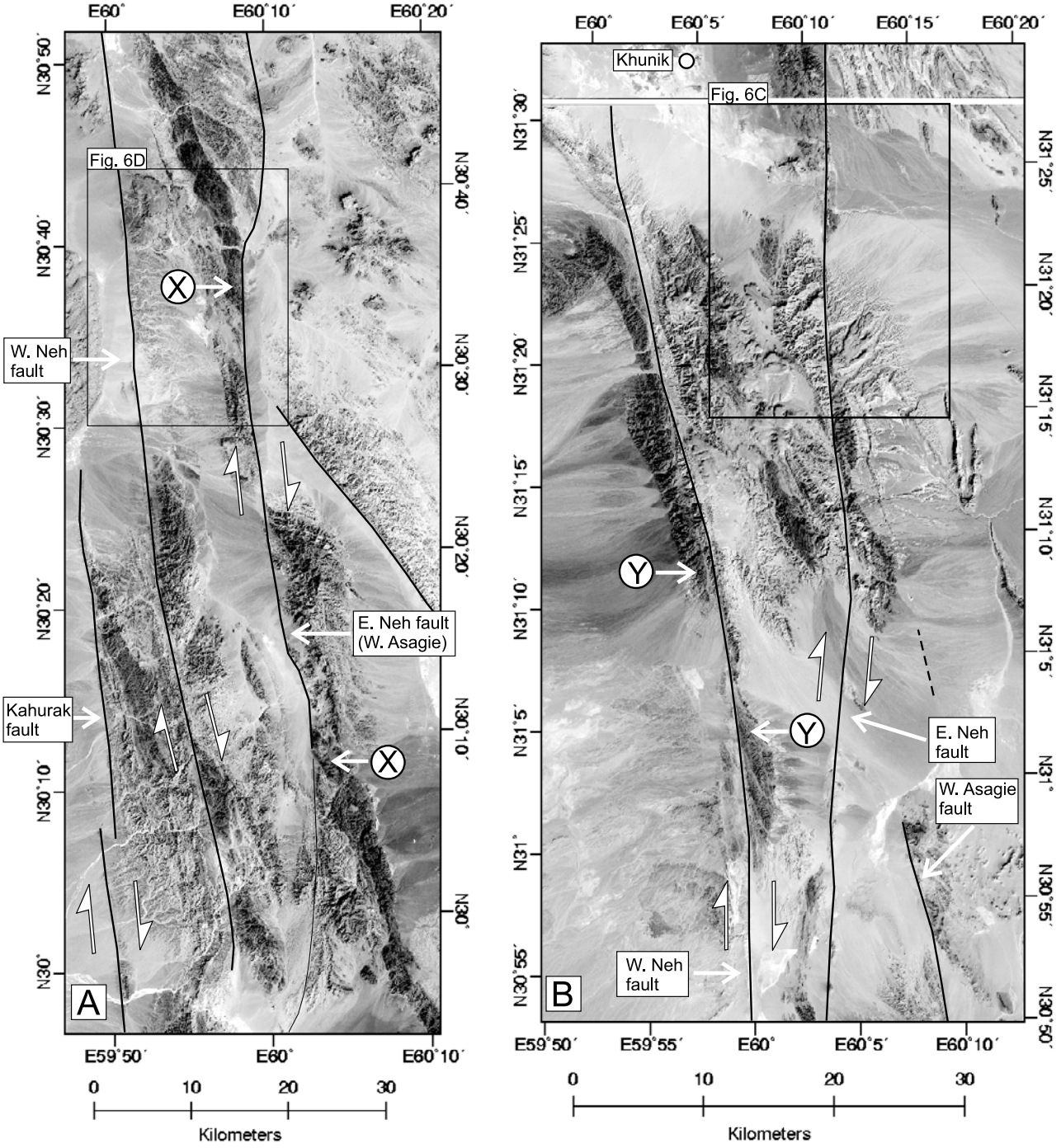

Figure 6. Landsat TM imagery of the East and West Neh faults. (a) The West Neh, East Neh (West Asagie segment), and Kahurak faults (see Figure 3 for location). A distinctive black band of peridotite is offset by ~50 km across the West Asagie fault (points marked X). The box shows the location of Figure 6d. (b) The East and West Neh faults (see Figure 3 for location). Mesozoic phyllite and ophiolitic material is displaced by ~10 km across the W. Neh fault (points marked Y). The box shows the region covered by Figure 6c. (c) Close-up of the East Neh fault where it is crossed by the Birjand-Zahedan road. The fault has a clear trace in alluvium and eastward flowing streams are displaced by ~5 km across the fault. (d) Close-up of the West Neh fault at the edge of the Dasht-e-Lut (left of picture). Uplift east of the fault has caused the incision of meandering rivers. The West Asagie fault can be seen on the right-hand side of the image.

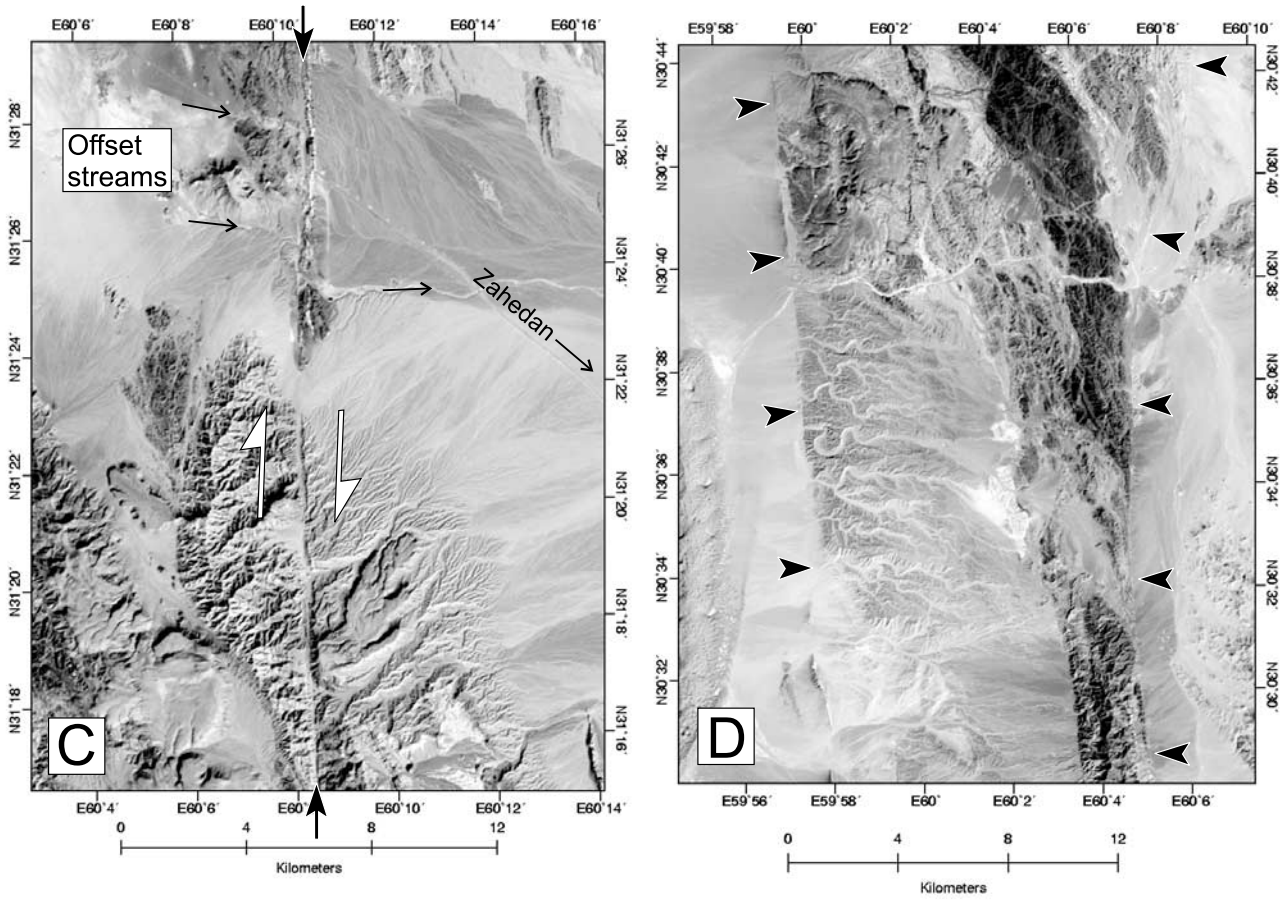

Figure 6. (continued)

involves increased components of shortening (Figure 3). However, at least 7 km of bedrock displacement is seen across one branch of the Purang fault at latitude 32°30′N (Figure 7) [*Sahandi*, 1992; *Vahdati-Daneshmand*, 1992], which is only one of several right-lateral faults at this latitude.

[23] We note that although restoration of the broad-scale topography of the East Iranian ranges would require at least 150 km of cumulative right-lateral shear along the line of the Kahurak and East Neh faults (Figure 3), a restoration of 150 km of right-lateral shear would not be compatible with the geology of the region, as it would align rocks of the Ratuk complex with those of the Neh complex (Figure 4a). These two deformed accretionary prisms are separate structural entities of different ages, that are separated by the Sefidabeh forearc basin [*Tirrul et al.*, 1983]. The topography is instead probably related to the overall structure of the Sistan suture zone, with almost pure strike-slip in the central parts, and substantial shortening components in the NW and SE that elevate the topography.

4.2. Cumulative Late Cenozoic Strain in Kerman Province: Western Dasht-e-Lut Margin

[24] *Walker and Jackson* [2002] investigated the total late Cenozoic slip on the Gowk fault, on the western margin of the Dasht-e-Lut (Figure 8a). The Gowk fault has generated several destructive earthquakes since 1981. Field observations and source parameters constrained by seismology indicate predominantly right-lateral strike-slip [e.g., *Berberian et al.*, 2001]. Realignment of offset bedrock and structural features and the reconstruction of drainage systems displaced by the fault imply a total cumulative right-lateral strike-slip of ~12 km, which *Walker and Jackson* [2002] use to suggest a slip-rate of only ~2.5 mm/yr if the faulting initiated at 5 Ma. A recent GPS experiment [*Vernant et al.*, 2004] suggest that rates of right-lateral shear to the south of the Gowk fault are higher (~6 mm/yr). An independent estimate of the slip-rate along the western Dasht-e-Lut margin is found on the Nayband fault to the north of the Gowk fault (Figure 8a), where ~2 Ma basalts are cut by the fault and displaced by ~3.2 km, yielding a slip-rate of ~1.5 mm/yr. The deficit is presumably taken up on the Kuh-banan fault (Figure 8a). The estimates of 2.5 to 6 mm/yr of right-lateral slip along the western margin of the Dasht-e-Lut are small compared to the ~15 mm/yr of right-lateral shear expected across eastern Iran [e.g., *Vernant et al.*, 2004].

[25] A total cumulative offset of substantially more than 12 km on the Gowk fault would introduce space problems

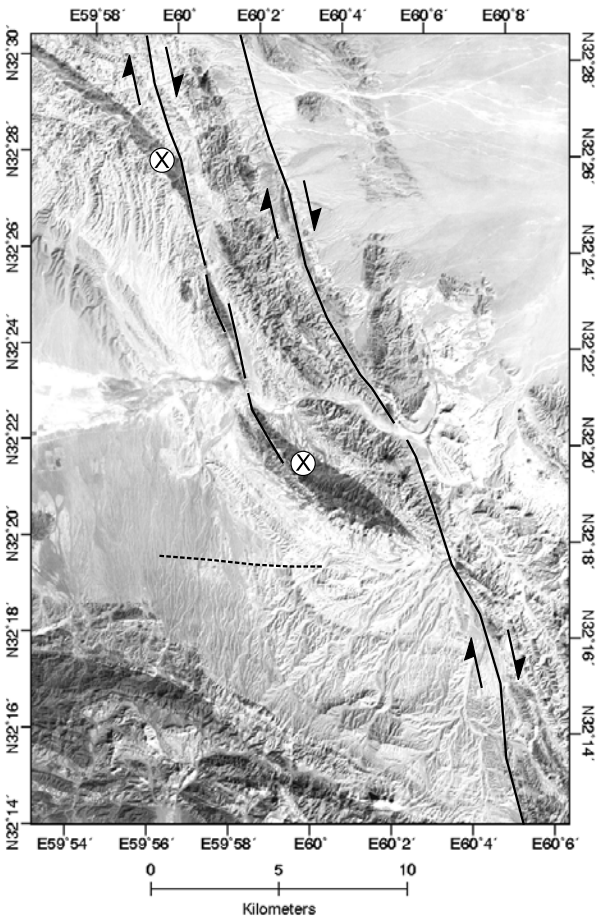

Figure 7. Landsat TM image of the Purang right-lateral strike-slip fault (see Figure 3 for location). Ultrabasic ophiolitic rocks are displaced by ~7 km (between points marked X) across the western strand of this fault.

that require a complete reorganization of topography, not only along the fault valley (e.g., the South Golbaf pull-apart depression, Figure 8b), but also in the mountain ranges that surround the Gowk fault (Figure 8a). We are therefore confident that the total offset is not significantly different from the ~12 km estimated by *Walker and Jackson* [2002]. A maximum cumulative strike-slip offset across the Gowk fault is given by the ~15 km displacement of the Gaznau river (Figure 8b; stream 7 in Figure 8 of *Walker and Jackson* [2002]). Although no definite lithological offsets can be demonstrated across the fault because of the differing geology of mountains to the east and west, there are indications that outcrops of dark-colored Cretaceous rocks to the west of the fault are brought into alignment with a thin sliver of material outcropping along the eastern margin of the South Golbaf depression (points marked X in Figure 8b).

[26] A proportion of the right-lateral shear on the Sabzevaran fault in the south (Figure 8a) may bypass the Gowk fault as shortening across thrust faults south of Kerman (Figure 8a). The elevated topography between latitudes 29°N and 29°30′N, with several parallel mountain ranges reaching up to 4420 m, and concentrated thrust faulting (Figure 8a), suggests intense active deformation. The northern end of the Sabzevaran fault and southern end of the Gowk fault overlap in this area, and a NW–SE alignment of folds indicate that a proportion of right-lateral shear is not localized across the Gowk fault. However, the apparently intense deformation at this junction between the Sabzevaran and Gowk faults may be caused by the anticlockwise rotation of strike-slip faults in central Iran, as discussed later (see section 5.3). As the Gowk fault is the only major structure west of the Dasht-e-Lut at this latitude that can directly transmit strain to the Nayband and Kuh-Banan faults to the north (Figure 8a), we are confident that the majority of deformation is localized across it.

4.3. Strike-Slip Faulting and Cumulative Strain in Central Iran

[27] In sections 4.1 and 4.2, the relative abundance of earthquake epicenters on the fault zones surrounding the Dasht-e-Lut show that the N–S faults accommodate right-lateral strike-slip and are active at the present day. The lack of seismicity within the Dasht-e-Lut and the deserts of central Iran have been used to infer that these regions are not deforming at the present day. Parts of central Iran west of the Nayband fault do, however, contain large strike-slip faults, the major ones being the Anar fault, the Deh Shir fault and the Great Kavir fault (the western extension of the Doruneh fault) (see Figure 1 and section 5.2). From the twentieth century earthquake distribution (Figure 2b), we might not expect these faults to be active, as they occur in flat, low-lying and apparently aseismic regions (Figures 1 and 2). However, the scarps associated with each of these faults appear remarkably fresh when observed using satellite imagery and in the field [e.g., *Berberian*, 1976]. Below, we describe the geomorphology of the Deh Shir, Anar, and Great Kavir faults and assess their role in the active tectonics of the region.

4.3.1. Deh Shir Fault

[28] The Deh Shir fault is shown in Figure 9. It is ~400 km long and has a roughly NNW trend. It is expressed clearly in satellite imagery (Figure 9) and on geological maps [e.g., *Aghanabati*, 1991], where it displaces bedrock units. Given the absence of earthquake mechanisms, the linear trend, N–S orientation, and right-lateral displacement of gravel fans (see later) indicate that the fault motion is predominantly right-lateral strike-slip. The total displacement is hard to estimate. However, the fault appears to displace Eocene-Oligocene volcanics within the Urumiyeh-Dokhtar zone (see Figure 1) by ~50 km right-laterally [*Berberian*, 1976; *Aghanabati*, 1991]. This large displacement may be misleading, as the small angle between the trend of these rock units and the fault makes it hard to quantify the true offset. We visited the Deh Shir fault at two locations, near its northern end at Na'in (Figures 9b, 10a, and 10b) and in the central part of the fault near the village of Deh Shir (Figures 9c and 10c). In both of these regions fault

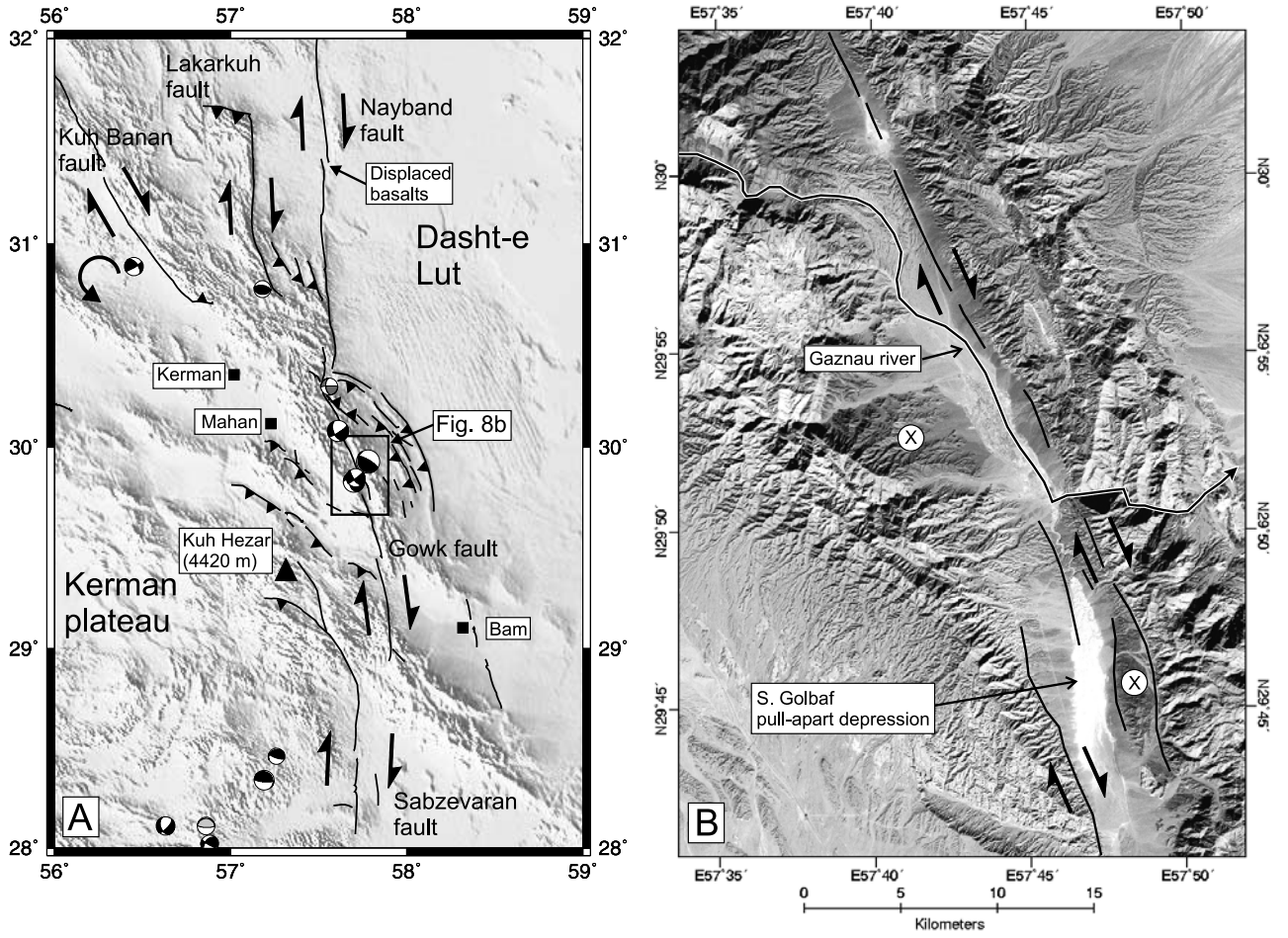

Figure 8. (a) GTOPO30 topography of the Kerman region centered on the Gowk fault (see Figure 1 for location). Fault plane solutions of shallow (<35 km) earthquakes are shown. Black solutions are events modeled using body waveforms (listed by *Jackson* [2001], *Walker* [2003], and *Talebian and Jackson* [2004]); dark gray represents events from the Harvard CMT catalogue with >70% double-couple component; light gray represents first-motion solutions [from *McKenzie*, 1972]. Zones of shortening and thrust faulting are seen both to the north of Kerman, where the Gowk fault splits into the Kuh-Banan, Lakar-Kuh, and Nayband faults, and south of Mahan, where NW–SE trending thrust faults occupy the region between the Sabzevaran and Gowk faults. These zones of intense deformation may be partly caused by rotation of crustal blocks, as marked by black arrows (see section 5.3). The box marks the location of Figure 8b. (b) Landsat TM image of the central part of the Gowk fault. Restoration of drainage and structural features indicate between 12 and 15 km of cumulative right-lateral displacement [*Walker and Jackson*, 2002]. Restoration of ~15 km of right-lateral slip aligns dark-colored lithologies (marked X), although it is not certain that the dark-colored rocks at either side of the fault are from a single displaced unit.

scarps are preserved at the surface, either in alluvium or in calcite-cemented sands (Figures 10a–10c) suggesting that some Quaternary movement has occurred. Similarly clear scarps in alluvium are seen in satellite imagery along the length of the fault.

4.3.2. Anar Fault

[29] A Landsat image of this fault is shown in Figures 11a–11c. It is ~200 km long. In the south, it appears to end in the mountains of Kuh-e-Mosahem, and in the north, it ends in an isolated zone of folding at ~32°45′N, 54°15′E (Figure 1). Continuous fault scarps in alluvium are seen along the southern part of the fault near Anar (Figure 11c). These scarps are downthrown to the west (Figure 11c) [*Berberian*, 1976]. The fault displaces sandstone units in a lower Cretaceous shale sequence exposed in the Kuh-e-Bafq mountain range, apparently by up to ~20 km right-laterally (between points marked X in Figure 11a) [*Nabavi*, 1970]. Several parallel fault strands are mapped in the Kuh-e-Kharanaq mountain range (Figure 11a), right-lateral displacements across individual strands are up to

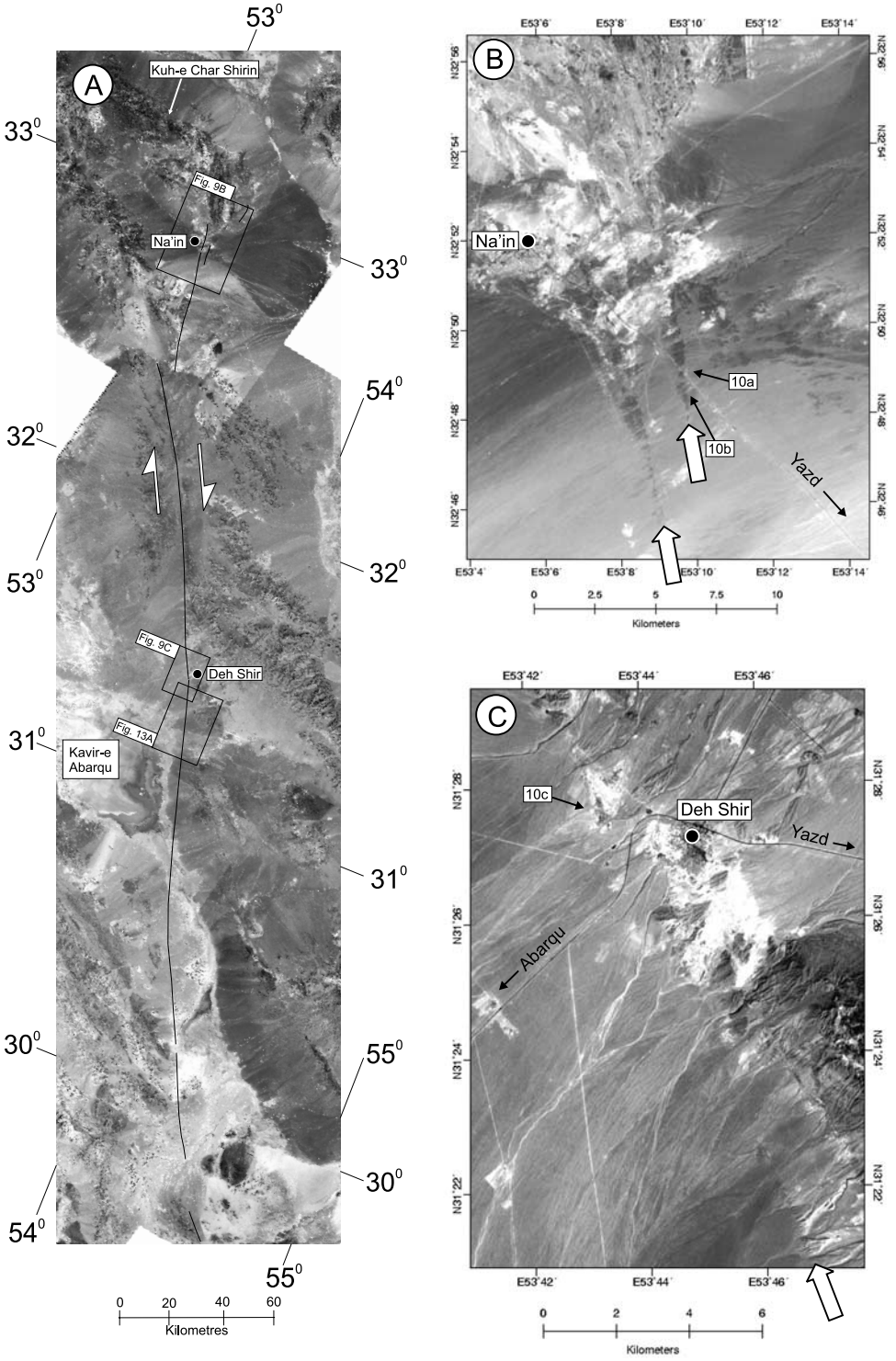

Figure 9. (a) Landsat TM mosaic of the Deh Shir fault in central Iran (see Figure 1 for location). The boxes show the regions covered by Figures 9b, 9c, and 13a. (b) Landsat TM+ close-up of east facing Deh Shir fault scarps at Na'in. The scarps are marked by white arrows. The arrow marks the location of the photo in Figure 10a. (c) West facing fault scarps at Deh Shir village. Incised rivers at the top left corner of the image are not displaced by the fault (see also Figure 13a).

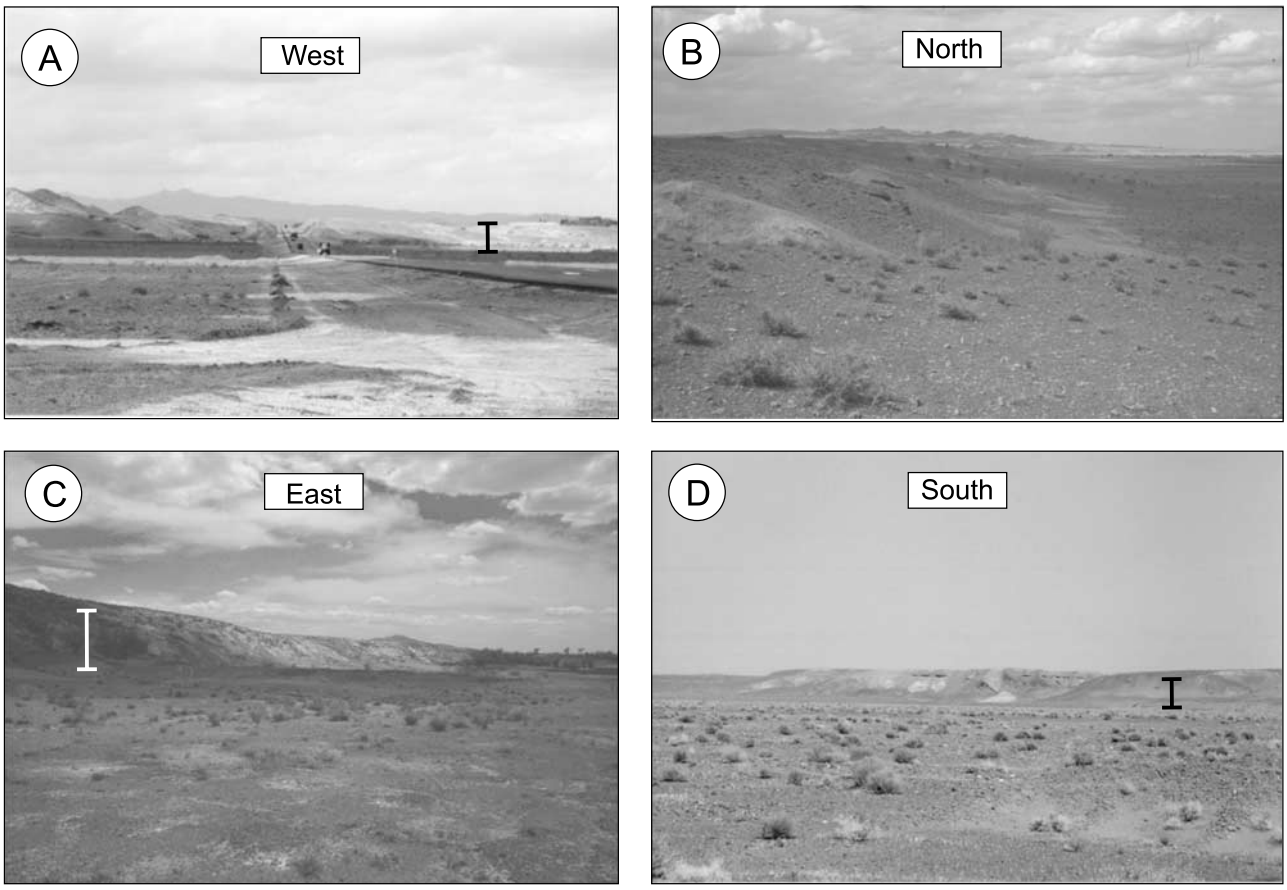

Figure 10. Photographs of fault scarps in central Iran. (a) The Deh Shir fault at Na'in (scarp ~15 m high). (b) View looking north along the fault scarp at Na'in. Kuh-e-Chah Shirin can be seen in the far distance; this marks the northern end of the Deh Shir fault. (c) The Deh Shir fault north of Deh Shir village (scarp ~10 m high). (d) The ~10 m high scarp of the Great Kavir fault near Jandaq.

5 km (between points marked Y in Figure 11b). The elongate, NNW–SSE trending Kuh-e-Bafq and Kuh-e-Kharanaq mountain ranges are bounded to the east by anticlines expressed in alluvial material (Figure 11a).

4.3.3. Great Kavir Fault

[30] This is a WSW trending left-lateral fault, and is the western continuation of the Doruneh fault (Figure 14; also see section 5.2). Little topography is associated with the fault, but it cuts through the flat salt pans of the Dasht-e-Kavir (Figures 12a and 12c). Toward the western end of the fault near Jandaq, the fault scarp is continuous and preserved in alluvial gravels and marls (Figures 12a and 12b). Further scarps in alluvium are observed south of the main trace near the village of Arusan (Figure 12a). We visited the fault where it is crossed by the Jandaq-Semnan road (Figure 12b), and observed a continuous ~10 m high scarp that might be the expression of the Great Kavir fault (Figure 10d).

4.3.4. Right-Lateral Faulting in Central Iran: Present-Day Activity

[31] The Deh Shir, Anar, and great Kavir faults of central Iran are all more than 100 km long and, if not slipping aseismically, may be capable of accumulating large amounts of elastic strain between earthquakes [*Scholz*, 1982]. Earthquake repeat times of several thousand years are possible if the slip-rates are relatively small, accounting for the lack of observed seismicity. An indication of the likely earthquake repeat time on the Deh Shir fault is seen in Figure 13. Figure 13 shows a river that incises through an abandoned alluvial fan south of Deh Shir village (see Figure 11a for location). The alluvial fan appears to be displaced right-laterally by at least 100 m along the Deh Shir fault (marked by arrows in Figure 13). Gravels exposed in the river cutting are also gently folded up to the fault trace (Figures 13b and 13c). However, the incised river channel itself does not show any indication of strike-slip displacement, indicating that no major surface displacements have occurred since the incision of this river, and suggesting that slip on the Deh Shir fault is not accommodated by aseismic creep.

[32] Changes in climate are often responsible for cycles of alluvial fan deposition and incision [e.g., *Jones et al.*, 1999; *Van der Woerd et al.*, 2002]. For example, climate records for southern (Mediterranean) Europe, suggest a postglacial shift to a relatively wet and warm climate

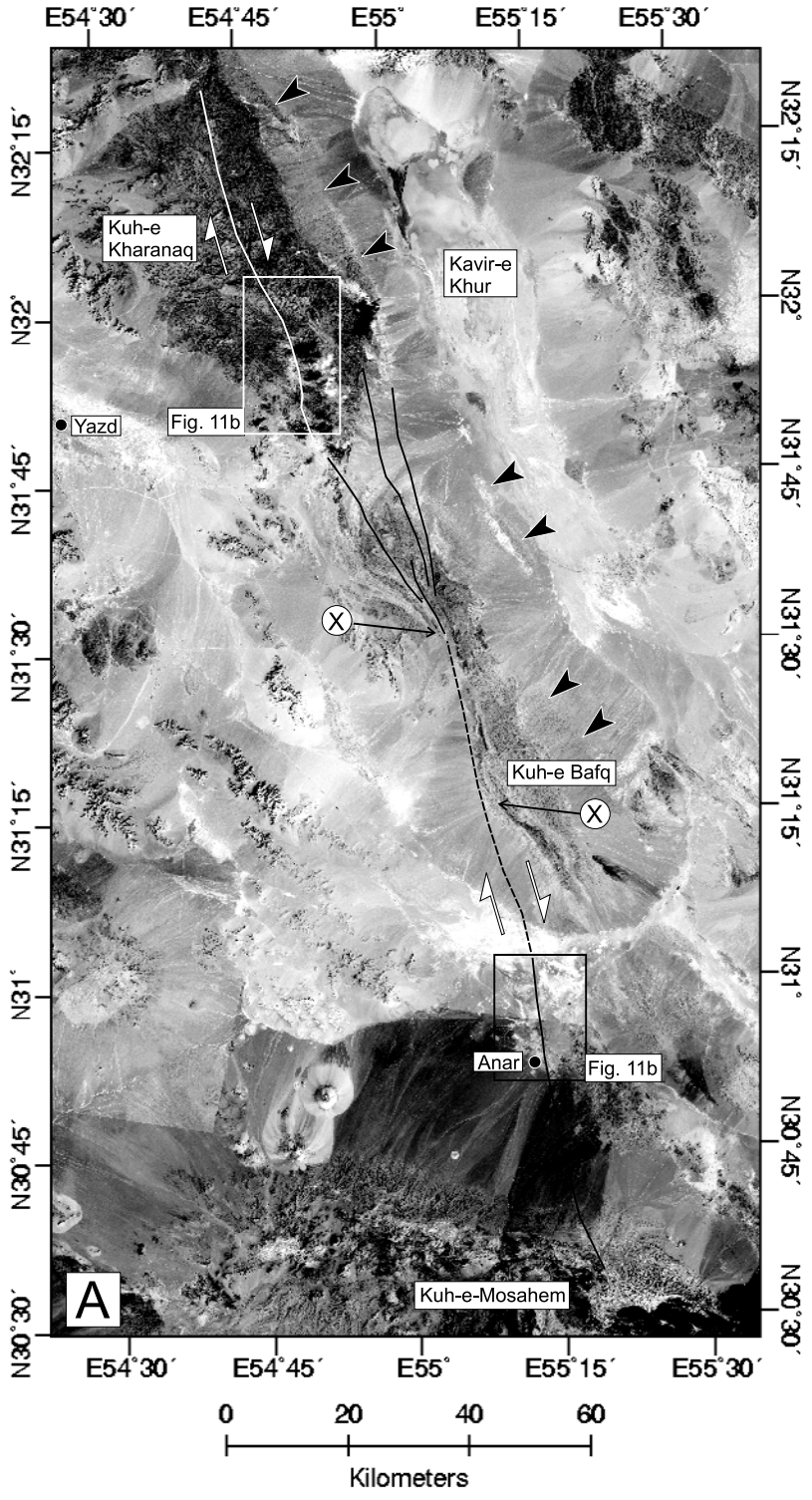

Figure 11. (a) Landsat TM+ mosaic of the Anar fault (see Figure 1 for location). The fault cuts through and displaces bedrock in Kuh-e-Kharanaq and Kuh-e-Bafq and forms a scarp in alluvium near Anar town. Points marked X are sandstone units within a sequence of Lower Cretaceous shales exposed in Kuh-e-Bafq, apparently displaced right-laterally by ~20 km [*Nabavi*, 1970]. Anticlines (marked by black arrows) run parallel to the Anar fault down the eastern margin of the mountain ranges. Boxes show the regions covered by Figures 11b and 11c. (b) Close-up view of one strand of the Anar fault in Kuh-e-Kharanaq. Bedrock is displaced by at least 5 km right-laterally (between points marked Y). (c) The Anar fault at Anar town. A clear scarp in alluvium runs down the center of the image.

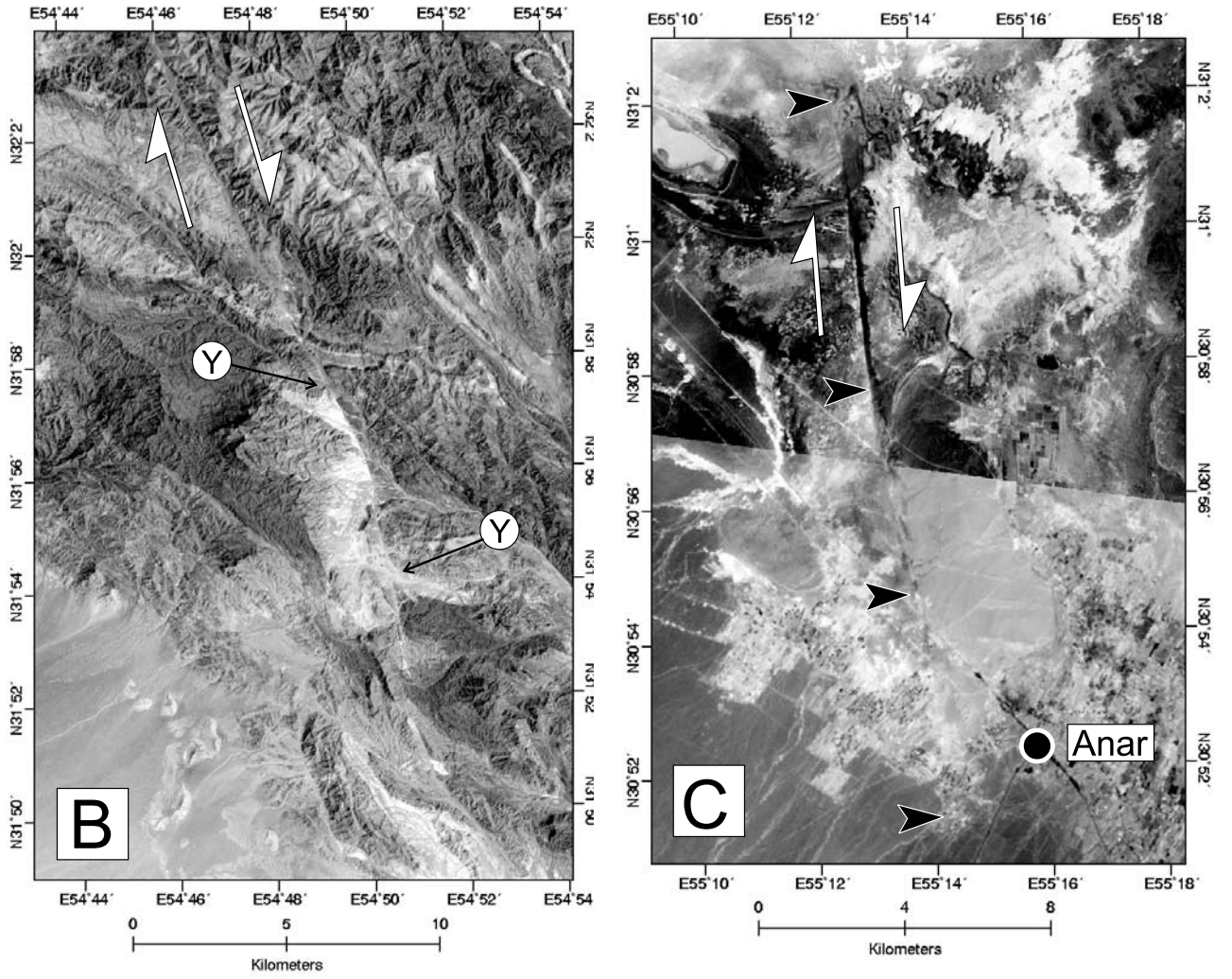

Figure 11. (continued)

~12,000 years ago. This change in climate has been interpreted as the cause of widespread exposure of fault planes in Greece [e.g., *Benedetti et al.*, 2002]. There is little constraint on the climate history of central Iran through the last few tens of thousands of years. However, dating of palaeolithic tools and ^{10}Be analysis of boulders within young river terraces in SE Iran yield a deposition age of between 5 and 9 Ka [*Regard*, 2003]. If we assume a similar climatic shift in central Iran, the abandonment of alluvial fans and river incision across the Deh Shir fault may date from as little as ~5000 years ago, indicating that no slip has occurred since this time. However, a fault ~100 km long can accumulate ~5 m of strain between earthquakes [e.g., *Scholz*, 1982]. The Deh Shir fault is ~400 km long and is unsegmented along much of its length (see Figure 9), and therefore it could easily accumulate over 5 m of strain between earthquakes. There is no reason to suppose that the Deh Shir fault is slipping rapidly at the present day, as it may be an old structure, dating from as early as ~12 Ma (see section 5.3) and much of the present-day deformation is concentrated along the eastern margin of Iran in Sistan (see section 2) [*Vernant et al.*, 2004]. A repeat time of more than 5000 years for large earthquakes on the Deh Shir fault does not seem unreasonable.

5. A Kinematic Model of Deformation in Eastern and Central Iran

[33] In the above sections, we have described the major right-lateral strike-slip fault systems of eastern and central Iran. We have also attempted to determine the total offset across each fault system. In the following sections we aim to describe the kinematics of active tectonics in eastern and central Iran (summarized in Figure 14). Our model is consistent with the data presented in this paper. However, there are not enough data to test several of the key assumptions and hypotheses, and the model is therefore speculative. We first consider the fault systems that are proven to be actively accommodating right-lateral shear

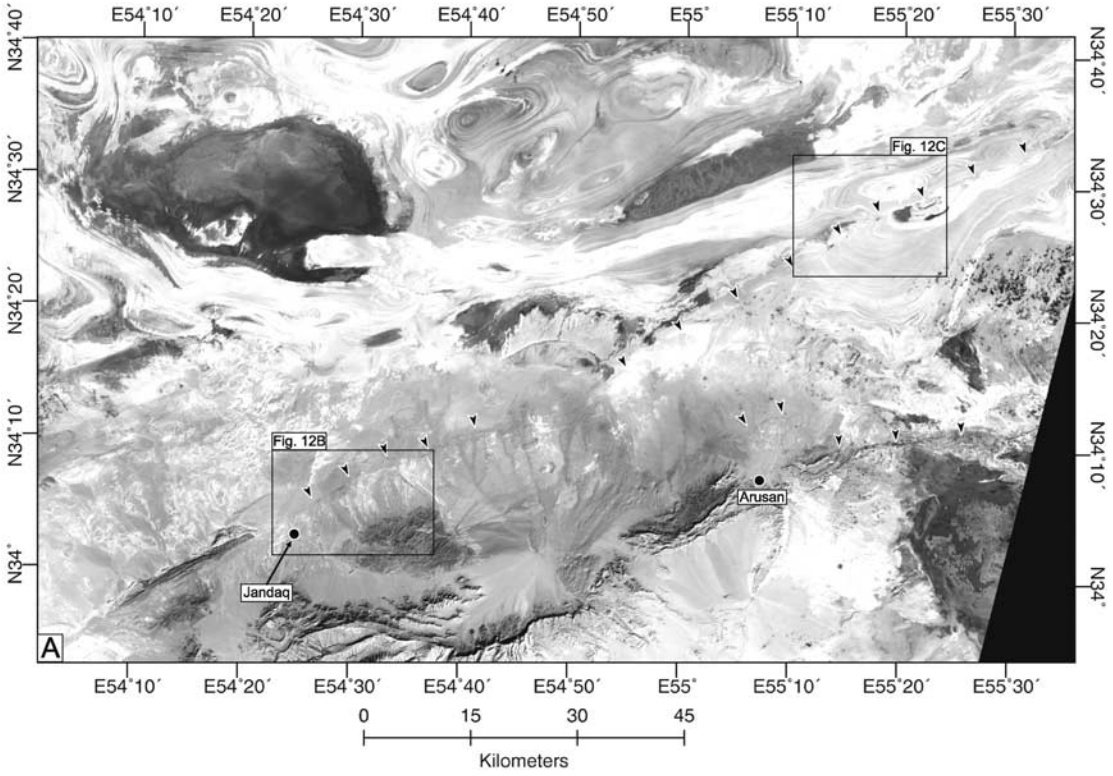

Figure 12. (a) Landsat TM image showing scarps of the Great Kavir fault in the Dasht-e-Kavir (see Figure 1 for location). Black arrows point to fault scarps. In the eastern part of the image, the fault cuts through evaporite and salt pan deposits. In the west of the image, scarps are preserved in alluvium. Boxes show the regions covered by Figures 12b and 12c. (b) Close-up of the region around Jandaq. A continuous, north facing scarp can be seen. The photograph in Figure 10d was taken where the scarp crosses the Semnan road. (c) Close-up of the Great Kavir fault in the Dasht-e-Kavir. The fault (marked by black arrows) displaces salt pan and underlying evaporite deposits.

between central Iran and Afghanistan, because of the occurrence of large instrumental and historical earthquakes. As we have no seismological evidence that the Anar, Deh Shir, and Great Kavir faults of central Iran are active at the present day, and as we know from GPS that large amounts of shortening do not occur across the central Iranian plateau [*Vernant et al.*, 2004], we do not consider these faults in our initial model.

5.1. Rates of Active Faulting Around the Dasht-e-Lut Desert

[34] Assuming that the present-day distribution of active faulting dates from ~3–7 Ma, and probably from 5–7 Ma because of the onset of shortening in the Kopet Dagh at ~5 Ma [*Lyberis and Manby*, 1999], we believe that the total north-south right-lateral shear expected in eastern Iran is about 75–105 km (see section 2). The cumulative fault offsets that we document for active right-lateral strike-slip faults around the Dasht-e-Lut account for this (although we cannot discount that some of the cumulative strain may be inherited from earlier phases of deformation). The combined fault offset of at least 70 km measured across the Sistan faults is much larger than the 12–15 km of cumulative right-lateral slip estimated for the Gowk fault to the west of the Dasht-e-Lut (see section 4.2 and *Walker and Jackson* [2002]). This implies that the strike-slip faults of the Sistan suture zone, taken as a whole, have accommodated the major part of the total right-lateral shear between Iran and Afghanistan. Assuming that the strain distribution has not varied through time, our kinematic model has implications for the estimation of regional seismic hazard, as the historical record of destructive earthquakes in Sistan is probably underrepresentative of the actual hazard from these structures [e.g., *Ambraseys and Melville*, 1982; *Ambraseys and Bilham*, 2003].

[35] The active north-south right-lateral strike-slip faults that surround the Dasht-e-Lut desert die out north of ~34°N. Above 34°N, the major active structures are east-west left-lateral faults, which are thought to accommodate right-lateral shear by rotating clockwise about a vertical axis [*Jackson and McKenzie*, 1984; *Jackson et al.*, 1995]. If our

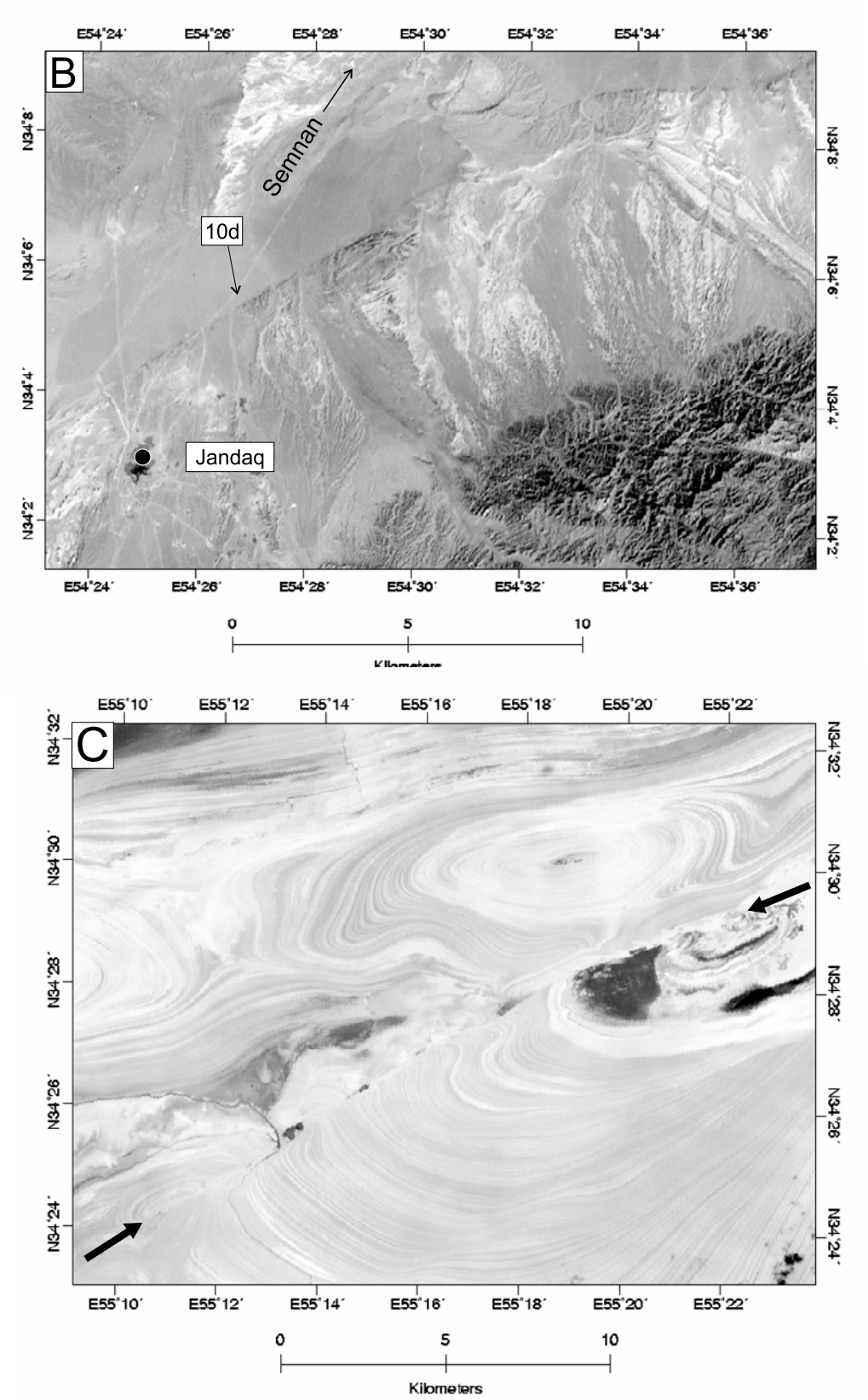

Figure 12. (continued)

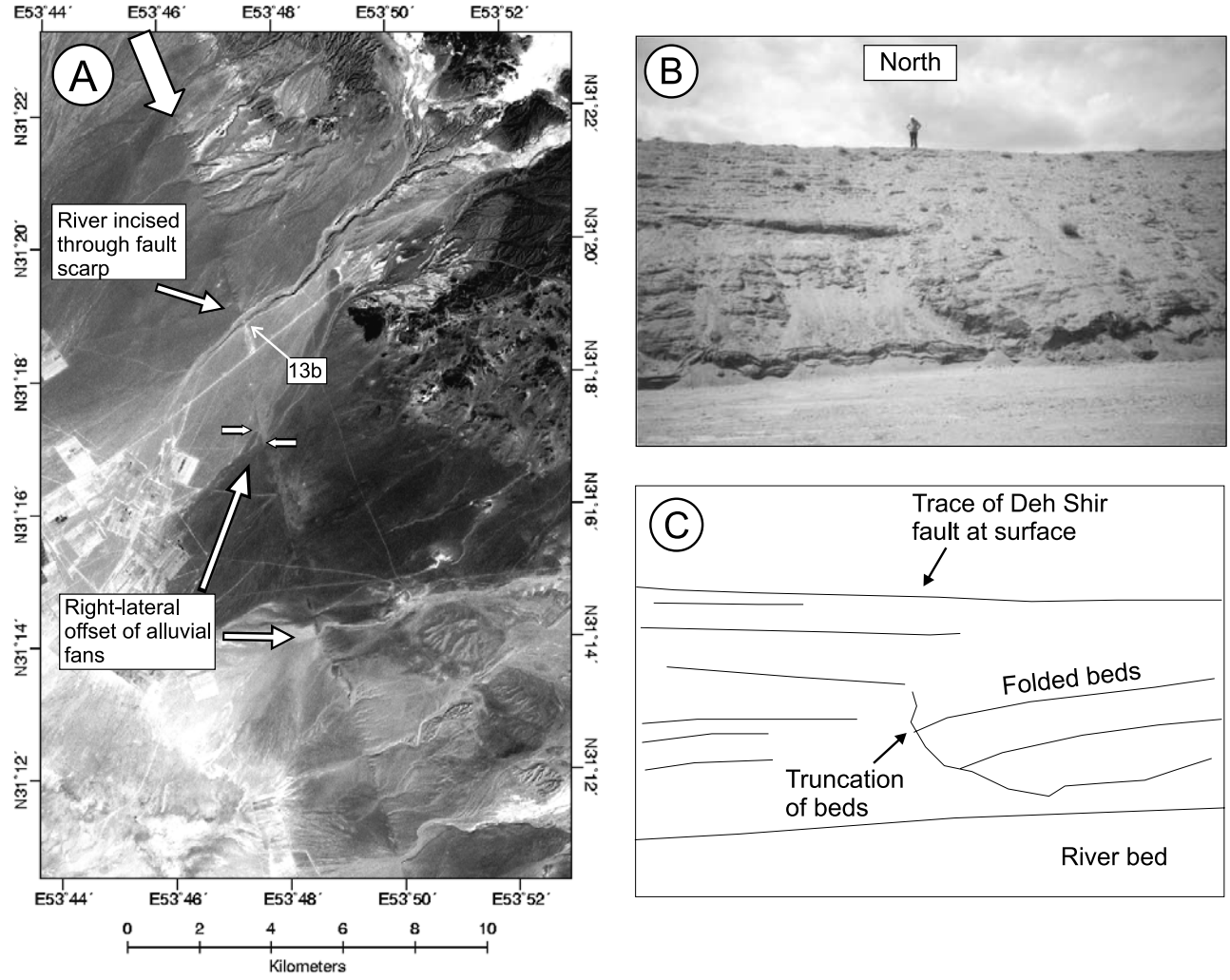

Figure 13. (a) Landsat TM+ view of the Deh Shir fault south of Deh Shir village (see Figure 9a for location). The fault scarp is marked by white arrows. Alluvial fans that cross the fault are apparently displaced right-laterally by a small amount. However, a river that incises through these fans is not displaced by the fault. The last fault activity must predate the river incision. (b) View looking into the north face of the incised river where it crosses the Deh Shir fault. The figure is standing at the fault trace. Gravel beds in the river cutting are folded and displaced at the fault. (c) Sketch of Figure 13b, highlighting the major relationships.

model is correct, it has important consequences for the development of the Dasht-e-Bayaz and Doruneh left-lateral faults that occur north of latitude 34°N (Figure 14). We consider the evidence for this in the next section.

5.2. Rotations and Left-Lateral Faulting in NE Iran

[36] The left-lateral Doruneh fault is one of the longest faults in Iran, stretching from the Afghan border to central Iran (the western part is often called the Great Kavir fault; see section 4.3.3), over a distance of ~600 km (Figures 1 and 15). The Doruneh fault must rotate clockwise about a vertical axis in order to accommodate N–S right-lateral shear [e.g., *Jackson and McKenzie*, 1984] seen in the GPS results [*Vernant et al.*, 2004]. There is a prominent curvature in the Doruneh fault trace, with a ESE–WNW strike in the east that bends round to a WSW–ESE strike west of ~58°E. A large component of shortening along the eastern part of the fault is demonstrated by parallel folds of the Jangal thrust fault system (Figure 15), that were probably responsible for a destructive earthquake in 1336 A.D. [*Ambraseys and Melville*, 1982]. West of ~56°30′E, the fault enters the Central Iranian Desert (the Dasht-e-Kavir); this part of the fault has no recorded earthquake activity and is discussed in section 4.3.3.

[37] The left-lateral Dasht-e-Bayaz fault occurs only east of ~58°E, in the region where the Doruneh fault has a ESE–WNW trend (Figure 15). *Walker et al.* [2004] use the

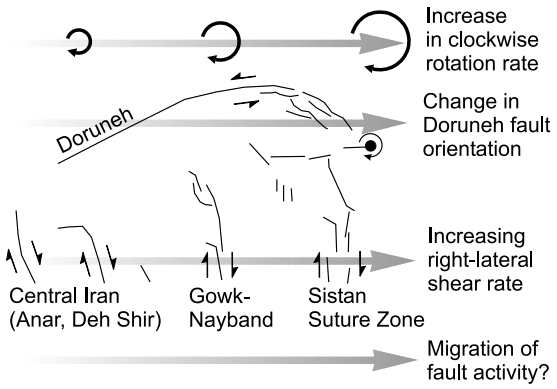

Figure 14. Cartoon showing the influence of an uneven distribution of N–S right-lateral shear on the fault systems of central Iran (Anar and Deh Shir), the Gowk-Nayband fault system, and the active faults of the Sistan suture zone. From west to east, an increase in cumulative N–S right-lateral shear is seen. This increase is reflected in the orientation of the Doruneh fault, as it rotates clockwise to accommodate the right-lateral shear: More rotation is required in the east than in the west. The concentration of present-day activity on active fault systems along the eastern margin of Iran may reflect a gradual eastward migration of activity away from central Iran over the last 5 to 10 Myr.

relatively small offset, the lack of cumulative fault topography, and the highly segmented nature of the fault to suggest that the Dasht-e-Bayaz fault may be quite young, and may not be a through-going structure at all, instead being composed of several small aligned faults that may eventually coalesce.

[38] The ESE–WNW trend of the Doruneh fault east of ~58°E may be caused by this eastern section of the Doruneh fault having undergone a greater amount of clockwise rotation than the parts of the fault west of 58°E. Both the Doruneh and Dasht-e-Bayaz faults converge on a point at the Afghan border (Figure 15). East of this point (marked in Figure 15) there are few indications of active faulting both in the geomorphology and in the seismicity (Figure 2), and it is possible that the faults rotate about this point. As the eastern part of the Doruneh fault is now close to perpendicular to the direction of regional shortening and has acquired a large component of shortening (the Jangal thrusts), it may no longer be able to accommodate further N–S right-lateral shear by clockwise rotation, and this situation may in turn have favored the initiation of the Dasht-e-Bayaz fault. The ~20° angle between the eastern part of the Doruneh fault and Dasht-e-Bayaz fault, measured from the Afghan border, corresponds to a N–S shear of ~70 km across the Sistan suture zone (Figure 15), which is similar to the cumulative bedrock offsets described in section 4.1. We note however, that as we have no palaeomagnetic constraints on the amounts of

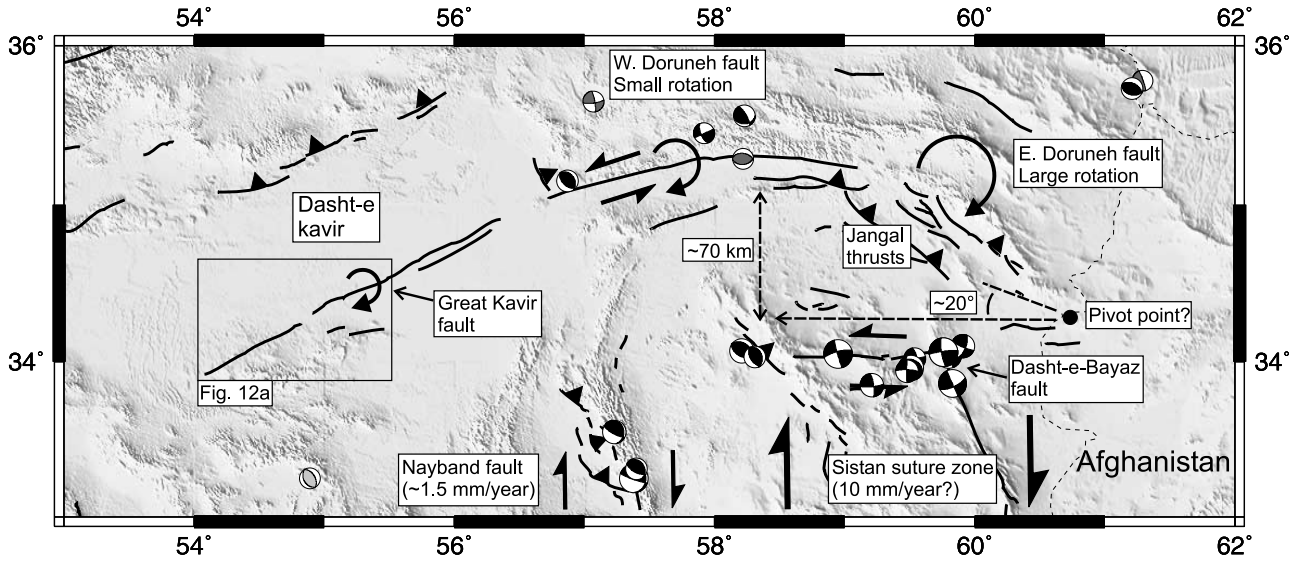

Figure 15. GTOPO30 topography of the Dasht-e-Bayaz and Doruneh faults in NE Iran (see Figure 1 for location). These left-lateral faults accommodate N–S right-lateral shear by clockwise rotation about vertical axes, possibly pivoting at a point close to the Afghan border (marked as a black circle). The prominent curvature of the Doruneh fault could be due to larger finite rotations in the eastern part of the fault, probably caused by a large proportion of the right-lateral shear being taken up across faults in the Sistan suture zone. Fault plane solutions of shallow (<35 km) earthquakes are shown. Black solutions are events modeled using body waveforms (listed by *Jackson* [2001], *Walker* [2003], and *Walker et al.* [2003, 2004]); dark gray represents events from the Harvard CMT catalogue with >70% double-couple component, light gray represents first-motion solutions (from *McKenzie* [1972]). The box marks the region covered by Figure 12a.

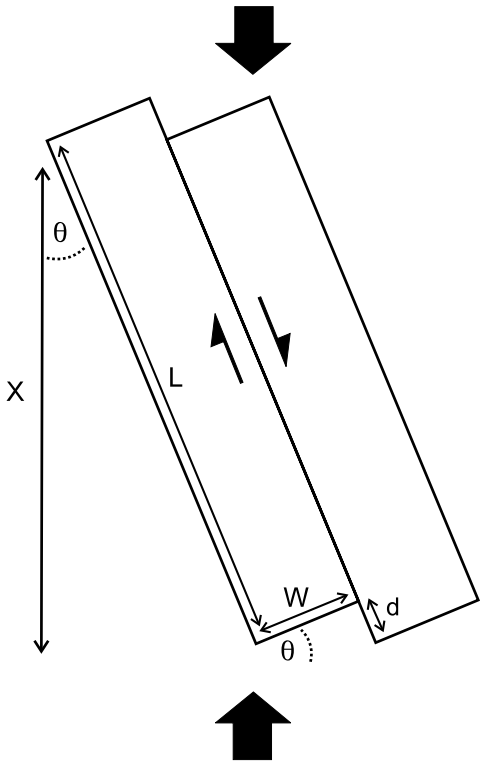

Figure 16. Cartoon showing how NNW–SSE right-lateral strike-slip faults in central Iran can accommodate N–S shortening by anticlockwise rotation about vertical axes. The block dimensions are taken from the length of the Deh Shir fault and the separation between the Deh Shir and Anar faults (see Figure 1). The ~50 km of right-lateral slip on the Deh Shir fault corresponds to an ~25° anticlockwise rotation (the angle between the faults in central Iran and the Nayband fault). The ~20 km of right-lateral slip on the Anar fault corresponds to a rotation of ~11°. Anticlockwise rotation of 10° to 20° can accommodate between 7 and 25 km of N–S shortening across central Iran.

vertical axis rotation, or of the initial orientation of the Doruneh fault, our arguments remain speculative. In particular, we have restricted our discussion to parts of the Doruneh fault directly north of the Dasht-e-Lut, across which ~15 mm/yr of right-lateral shear is determined from GPS measurements (Figure 15). We use the ~20° angle between the eastern Doruneh fault and the Dasht-e-Bayaz fault to infer a total clockwise rotation of ~20°. If we were also to consider the orientation of the western extension of the Doruneh fault (the Great Kavir fault, Figure 15), we would have to infer greater amounts of clockwise rotation.

5.3. Implications for Faulting and Earthquakes in Central Iran

[39] Our kinematic model has focused until now on the fault systems surrounding the Dasht-e-Lut, as these fault systems have produced many earthquakes, and must accommodate a combined total of ~15 mm/yr of right lateral shear between central Iran and Afghanistan. However, in section 4.3 we suggested from observations of satellite imagery and fieldwork that the Deh Shir, Anar, and Great Kavir faults of central Iran may be active at the present day.

[40] We cannot be certain that the large (>10 km) bedrock offsets on the Deh Shir and Anar faults are related solely to the present-day tectonic configuration. Considerable deformation and shortening is known to have occurred in the central Iranian plateau between 5 and 12 Ma [e.g., *Şengör and Kidd*, 1979; *Şengör*, 1990; *Allen et al.*, 2004], and these faults may have been active during this time. It is even possible that the major fault activity has migrated eastward away from central Iran, with the faults surrounding the Dasht-e-Lut becoming more important over the last ~5 to 7 Ma (see Figure 14). However, the geomorphology of the Deh Shir, Anar, and Great Kavir faults suggest that they do retain some degree of present-day activity, and so have the potential to move in earthquakes.

[41] If the faults in central Iran do retain some degree of present-day activity, they must play a role in accommodating Arabia-Eurasia convergence. The Deh Shir and Anar strike-slip faults of central Iran appear to have cumulative displacements of over 10 km. However, the ~75–105 km of right-lateral shear expected in eastern Iran over the last ~5 to 7 Myr can be accounted for by the total cumulative offsets of strike-slip faults that border the Dasht-e-Lut. The Deh-shir and Anar faults, although major structures, do not clearly link at either their northern or southern ends with other throughgoing faults and so probably do not accommodate throughgoing right-lateral shear between east and central Iran. The Deh Shir fault is located directly north of the Zagros mountains. Therefore, if it accommodates right-lateral shear between east and central Iran, this shear will result in a strain gradient between the parts of the Zagros to the east and the west of the intersection with the Deh Shir fault, of which there is no evidence.

[42] A possible explanation for present-day activity on the faults of central Iran is that a small amount of shortening is accommodated in central Iran. We know from GPS that the shortening across central Iran is not more than

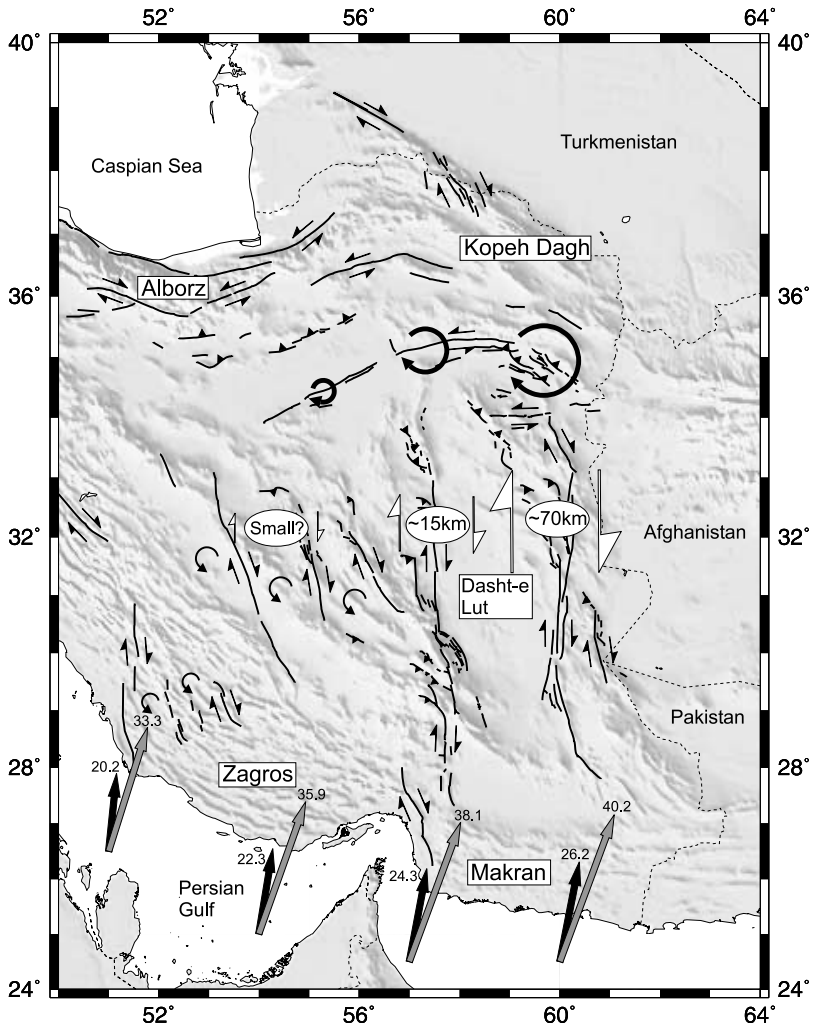

Figure 17. Fault map of central and eastern Iran, summarizing the ideas put forward in this paper. See Figure 1 for detailed geographical information. The curvature of the Doruneh fault, limited extent of the Dasht-e-Bayaz fault, and cumulative displacements estimated across the right-lateral fault systems to the east and west of the Dasht-e-Lut all indicate that a large proportion of the N–S right-lateral shear between central Iran and Afghanistan is accommodated along the eastern margin of the Dasht-e-Lut (represented by large white arrows). This concentration of shear results in the relatively rapid clockwise rotation of fault bounded blocks north of ~34°N (large black arrows). Although there is little seismicity in central Iran, the Great Kavir, Deh Shir, and Anar strike-slip faults may retain a small degree of activity, possibly to accommodate a small amount of shortening across central Iran by clockwise rotation, which in turn causes activity and clockwise rotation on the Great Kavir fault. Although the model proposed here is consistent with the available information, many of the major ideas remain speculative.

~2 mm/yr [*Vernant et al.*, 2004]. N–S shortening could be achieved by anticlockwise rotation about vertical axes of crustal blocks bounded by the right-lateral Deh Shir and Anar strike-slip faults, although without palaeomagnetic data this suggestion is speculative. The right-lateral strike-slip faults are up to ~400 km in length and ~100 km apart (Figure 1) and define fault-bounded blocks of these dimensions (Figure 16). The rigid-block model in Figure 16 is almost certainly an oversimplification, as it does not account for diffuse deformation within the blocks that is likely to occur, but is a useful approach for determining the approximate scale of displacements associated with the rotation. Anticlockwise rotation of the fault-bounded blocks in Figure 16 of 10°–20° will accommodate 7–25 km of total shortening across central Iran and can account both for the apparent present-day activity of the fault systems in central Iran and for the cumulative displacements across the faults (Figure 16). If the blocks are shorter (e.g., ~200 km for the Anar fault), the cumulative displacements of more than 10 km can be produced by less north-south shortening. Also, as suggested earlier, some of the cumulative bedrock displacement may predate the present-day tectonics.

[43] Anticlockwise block rotation might account for the splitting of the Gowk fault at its northern end into the

Nayband, Lakar-Kuh and Kuh-Banan faults (Figure 8a). The Kuh-Banan fault appears to end in an isolated region of folding (~32°N, 56°E), and has a NW–SE orientation closer to that of the Deh Shir and Anar faults than the overall N–S orientation of the faults that border the Dasht-e-Lut. The Kuh-Banan fault may be accommodating shortening by anticlockwise rotation (Figures 1 and 8a). This configuration would account for the apparently intense deformation in the junction between the Kuh-Banan, Nayband, and Gowk faults, and also to the south of Kerman (section 4.2 and Figure 8a), as block rotation will lead to shortening where the blocks abut the apparently rigid Lut.

6. Conclusions

[44] Relating the late Cenozoic strain distribution to the present-day rates and styles of deformation in eastern and central Iran has implications both for the estimation of seismic hazard and the active tectonics of Iran (Figures 14 and 17). The situation we describe may be wrong in detail, as we have assumed that the strain distribution is unchanged from the initiation of the present-day tectonic configuration. We have also had to assume that this configuration started ~5 to 7 Myr ago, on the basis of geological information from the surrounding deforming regions (see section 2), and yet it is roughly consistent with what we know of the present-day rates of shear in eastern Iran (see section 2). In the near future, we may have better estimates of the age of the active faults, GPS studies will constrain the present-day strain distribution, and palaeoseismological and geochronological studies will provide detailed information on the slip rates across individual fault zones. Thus the information from geomorphology, satellite imagery, and seismicity in this paper provides a framework to which later, more detailed, work can be added.

[45] **Acknowledgments.** We would like to thank M. T. Khorehei and M. Qorashi of the Geological Survey of Iran in Tehran for their continued support of our work. The catalogue of historical earthquakes in Figure 2b was kindly provided by N. Ambraseys. Several of the figures were produced using the Generic Mapping Tools software of *Wessel and Smith* [1998]. R. W. was funded by a NERC studentship. This work was supported by the NERC Centre for the Observation and Modelling of Earthquakes and Tectonics (COMET). The original manuscript was improved by detailed reviews from Gary Axen, Doug Walker, and an anonymous reviewer. Comments from Mark Allen, Philip England, and Dan McKenzie also helped to shape the final paper. This is Cambridge Earth Science contribution 7424.

References

Aghanabati, A. (1991), Geological quadrangle map of Iran, Daryacheh-ye-Hamun sheet (L10), scale 1:250,000, Geol. Surv. of Iran, Tehran.

Allen, M. B., S. Jones, A. Ismail-Zadeh, M. D. Simmons, and L. Anderson (2002), Onset of subduction as the cause of rapid Pliocene-Quaternary subsidence in the South Caspian basin, *Geology*, *30*, 775–778.

Allen, M., J. Jackson, and R. Walker (2004), Late Cenozoic reorganization of the Arabia-Eurasia collision and the comparison of short-term and long-term deformation rates, *Tectonics*, *23*, TC2008, doi:10.1029/2003TC001530.

Ambraseys, N. N., and R. Bilham (2003), Earthquakes in Afghanistan, *Seismol. Res., Lett.*, *74*, 107–123.

Ambraseys, N. N., and J. A. Jackson (1998), Faulting associated with historical and recent earthquakes in the eastern Mediterranean region, *Geophys. J. Int.*, *133*, 390–406.

Ambraseys, N. N., and C. P. Melville (1982), *A History of Persian Earthquakes*, Cambridge Univ. Press, New York.

Ambraseys, N. N., and J. S. Tchalenko (1969), The Dasht-e-Bayas (Iran) earthquake of August 31, 1968: A field report, *Bull. Seismol. Soc. Am.*, *59*, 1751–1792.

Axen, G. J., P. S. Lam, M. Grove, D. F. Stockli, and J. Hassanzadeh (2001), Exhumation of the west-central Alborz Mountains, Iran, Caspian subsidence, and collision-related tectonics, *Geology*, *29*, 559–562.

Behruzi, A. (1995), Geological quadrangle map of Iran, Zahedan sheet (L11), scale 1:100,000, Geol. Surv. of Iran, Tehran.

Benedetti, L., R. Finkel, D. Papanastassiou, G. King, R. Armijo, F. Ryerson, D. Farber, and F. Flerit (2002), Post-glacial slip history of the Sparta fault (Greece) determined by ^{36}Cl cosmogenic dating: Evidence for non-periodic earthquakes, *Geophys. Res. Lett.*, *29*(8), 1246, doi:10.1029/2001GL014510.

Berberian, M. (1976), Contribution to the seismotectonics of Iran (part II), *Rep. 39*, Geol. Surv. of Iran, Tehran.

Berberian, M. (1981), Active faulting and tectonics of Iran, in *Zagros, Hindu Kush, Himalaya: Geodynamic Evolution*, *Geodyn. Ser.*, vol. 3, edited by H. K. Gupta and F. M. Delany, pp. 33–69, AGU, Washington, D. C.

Berberian, M., and G. C. P. King (1981), Towards a palaeogeography and tectonic evolution of Iran, *Can. J. Earth Sci.*, *18*, 210–265.

Berberian, M., and R. S. Yeats (1999), Patterns of historical earthquake rupture in the Iranian Plateau, *Bull. Seismol. Soc. Am.*, *89*, 120–139.

Berberian, M., J. A. Jackson, M. Qorashi, M. M. Khatib, K. Priestley, M. Talebian, and M. Ghafuri-Ashtiani (1999), The 1997 May 10 Zirkuh (Qa'enat) earthquake (M_w 7.2): Faulting along the Sistan suture zone of eastern Iran, *Geophys. J. Int.*, *136*, 671–694.

Berberian, M., J. A. Jackson, M. Qorashi, M. Talebian, M. M. Khatib, and K. Priestley (2000), The 1994 Sefidabeh earthquakes in eastern Iran: Blind thrusting and bedding-plane slip on a growing anticline, and active tectonics of the Sistan suture zone, *Geophys. J. Int.*, *142*, 283–299.

Berberian, M., J. A. Jackson, E. Fielding, B. Parsons, K. Priestley, M. Qorashi, M. Talebian, R. Walker, T. J. Wright, and C. Baker (2001), The 1998 March 14 Fandoqa earthquake (M_w 6.6) in Kerman province, southeast Iran: Re-rupture of the 1981 Sirch earthquake fault, triggering of slip on adjacent thrusts and the active tectonics of the Gowk fault zone, *Geophys. J. Int.*, *146*, 371–398.

Camp, V. E., and R. J. Griffis (1982), Character, genesis and tectonic setting of igneous rocks in the Sistan suture zone, eastern Iran, *Lithos*, *3*, 221–239.

Chu, D., and R. G. Gordon (1998), Current plate motions across the Red Sea, *Geophys. J. Int.*, *135*, 313–328.

DeMets, C., R. G. Gordon, D. F. Argus, and S. Stein (1994), Effect of recent revisions to the geomagnetic reversal time scale on estimates of current plate motions, *Geophys. Res. Lett.*, *21*, 2191–2194.

Devlin, W. J., J. M. Cogswell, G. M. Gaskins, G. H. Isaksen, D. M. Pitcher, D. P. Puls, K. O. Stanley, and G. R. T. Wall (1999), South Caspian basin: Young, cool, and full of promise, *GSA Today*, *9*, 1–9.

Dewey, J. F., M. R. Hempton, W. S. F. Kidd, F. Saroglu, and A. M. C. Şengör (1986), Shortening of continental lithosphere: The neotectonics of eastern Anatolia, a young collision zone, *Geol. Soc. Spec. Publ.*, *19*, 3–36.

Eftekhar-Nezhad, J. (1990), Geological quadrangle map of Iran, Khunik sheet (8052), scale 1:100,000, Geol. Surv. of Iran, Tehran.

Eftekhar-Nezhad, J. (1991), Geological quadrangle map of Iran, Kuh-e-Seyasteragi sheet (8051), scale 1:100,000, Geol. Surv. of Iran, Tehran.

Engdahl, E. R., R. van der Hilst, and R. Buland (1998), Global teleseismic earthquake relocation with improved travel times and procedures for depth determination, *Bull. Seismol. Soc. Am.*, *88*, 722–743.

Falcon, N. L. (1974), Southern Iran: Zagros mountains, *Geol. Soc. Spec. Publ.*, *4*, 199–211.

Freund, R. (1970), Rotation of strike slip faults in Sistan, southeast Iran, *J. Geol.*, *78*, 188–200.

Haghipour, A., and M. Amidi (1980), The November 14 to December 25, 1979 Ghaenat earthquakes of northwest Iran and their tectonic implications, *Bull. Seismol. Soc. Am.*, *70*, 1751–1757.

Hessami, K. (2002), Tectonic history and present-day deformation in the Zagros fold-thrust belt, Ph.D. thesis, Univ. of Uppsala, Uppsala, Sweden.

Jackson, J. (1992), Partitioning of strike-slip and convergent motion between Eurasia and Arabia in eastern Turkey and the Caucasus, *J. Geophys. Res.*, *97*, 12,471–12,479.

Jackson, J. (2001), Living with earthquakes: Know your faults, *J. Earthquake Eng.*, *5*, 5–123.

Jackson, J., and D. McKenzie (1984), Active tectonics of the Alpine-Himalayan belt between western Turkey and Pakistan, *Geophys. J. R. Astron. Soc.*, *77*, 185–264.

Jackson, J., and D. McKenzie (1988), The relationship between plate motions and seismic moment tensors, and the rates of active deformation in the Mediterranean and Middle East, *Geophys. J.*, *93*, 45–73.

Jackson, J. A., J. Haines, and W. Holt (1995), The accommodation of Arabia-Eurasia plate conver-

gence in Iran, *J. Geophys. Res.*, *100*, 15,205–15,219.

Jackson, J., K. Priestly, M. Allen, and M. Berberian (2001), Active tectonics of the South Caspian basin, *Geophys. J. Int.*, *148*, 214–245.

Jestin, F., P. Huchon, and J. M. Gaulier (1994), The Somalia plate and the East African Rift System: Present-day kinematics, *Geophys. J. Int.*, *116*, 637–654.

Jones, S. J., L. E. Frostick, and T. R. Astin (1999), Climatic and tectonic controls on fluvial incision and aggradation in the Spanish Pyrenees, *J. Geol. Soc. London*, *156*, 761–769.

Lyberis, N., and G. Manby (1999), Oblique to orthogonal convergence across the Turan Block in the post-Miocene, *AAPG Bull.*, *83*, 1135–1160.

McCall, G. J. H. (1996), The inner Mesozoic to Eocene ocean of south and central Iran and associated microcontinents, *Geotectonics*, *29*, 490–499.

McKenzie, D. (1972), Active tectonics of the Mediterranean region, *Geophys. J. R. Astron. Soc.*, *30*, 109–185.

McQuarrie, N., J. M. Stock, C. Verdel, and B. P. Wernicke (2003), Cenozoic evolution of Neotethys and implications for the causes of plate motions, *Geophys. Res. Lett.*, *30*, 2036, doi:10.1029/2003GL017992.

Molnar, P., and P. Tapponnier (1975), Cenozoic tectonics of Asia: Effects of a continental collision, *Science*, *189*, 419–426.

Nabavi, M. H. (1970), Geological quadrangle map of Iran, Yazd sheet (H9), scale 1:250,000, Geol. Surv. of Iran, Tehran.

Nowroozi, A. A., and A. Mohajer-Ashjai (1985), Fault movements and tectonics of eastern Iran: Boundaries of the Lut plate, *Geophys. J. R. Astron. Soc.*, *83*, 215–237.

Regard, V. (2003), Variations temporelle et spatiale de la transition subduction-collision: Tectonique de la transition Zagros-Makran (Iran) et modelisation analogique, Ph.D. thesis, Univ. d'Aix Marseille III, Aix en Provence, France.

Sahandi, M. R. (1992), Geological quadrangle map of Iran, Dehsalm (Chah Vak) sheet (K9), scale 1:250,000, Geol. Surv. of Iran, Tehran.

Saidi, A. (1989), Geological quadrangle map of Iran, Chehelkureh sheet (8050), scale 1:100,000, Geol. Surv. of Iran, Tehran.

Scholz, C. (1982), Scaling laws for large earthquakes: Consequences for physical models, *Bull. Seismol. Soc. Am.*, *72*, 1–14.

Sella, G. F., T. H. Dixon, and A. Mao (2002), REVEL: A model for Recent plate velocities from space geodesy, *J. Geophys. Res.*, *107*(B4), 2081, doi:10.1029/2000JB000033.

Şengör, A. M. C. (1990), A new model for the late Palaeozoic-Mesozoic tectonic evolution of Iran and implications for Oman, in *The Geology and Tectonics of the Oman Region*, edited by A. H. F. Robertson, M. P. Searle, and A. C. Ries, *Geol. Soc. Spec. Publ.*, *49*, 797–831.

Şengör, A. M. C., and W. S. F. Kidd (1979), Post-collisional tectonics of the Turkish-Iranian plateau and a comparison with Tibet, *Tectonophysics*, *55*, 361–376.

Talebian, M., and J. Jackson (2002), Offset on the Main Recent Fault of NW Iran and implications for the late Cenozoic tectonics of the Arabia-Eurasia collision zone, *Geophys. J. Int.*, *150*, 422–439.

Tatar, M., D. Hatzfeld, J. Martinod, A. Walpersdorf, M. Ghafori-Ashtiany, and J. Chéry (2002), The present-day deformation of the central Zagros from GPS measurements, *Geophys. Res. Lett.*, *29*(19), 1927, doi:10.1029/2002GL015427.

Tirrul, R., I. R. Bell, R. J. Griffis, and V. E. Camp (1983), The Sistan suture zone of eastern Iran, *Geol. Soc. Am. Bull.*, *94*, 134–150.

Vahdati-Daneshmand, F. (1992), Geological quadrangle map of Iran, Birjand sheet (K8), scale 1:250,000, Geol. Surv. of Iran, Tehran.

Van der Woerd, J., P. Tapponnier, F. J. Ryerson, A.-S. Meriaux, B. Meyer, Y. Gaudemer, R. C. Finkel, M. W. Caffee, Z. Guoguang, and X. Zhiqin (2002), Uniform postglacial slip-rate along the central 600 km of the Kunlun fault (Tibet), from ^{26}Al, ^{10}Be, and ^{14}C dating of riser offsets, and climatic origin of the regional morphology, *Geophys. J. Int.*, *148*, 356–388.

Vernant, P., et al. (2004), Present-day crustal deformation and plate kinematics in the Middle East constrained by GPS measurements in Iran and northern Oman, *Geophys. J. Int.*, *157*, 381–398.

Walker, R. T. (2003), Active faulting and tectonics of eastern Iran, Ph.D. thesis, Univ. of Cambridge, Cambridge, UK.

Walker, R., and J. Jackson (2002), Offset and evolution of the Gowk fault, S. E. Iran: A major intra-continental strike-slip system, *J. Struct. Geol.*, *24*, 1677–1698.

Walker, R., J. Jackson, and C. Baker (2003), Surface expression of thrust faulting in eastern Iran: Source parameters and surface deformation of the 1978 Tabas and 1968 Ferdows earthquake sequences, *Geophys. J. Int.*, *152*, 749–765.

Walker, R., J. Jackson, and C. Baker (2004), Active faulting and seismicity of the Dasht-e-Bayaz region, eastern Iran, *Geophys. J. Int.*, *157*, 265–282.

Wellman, H. W. (1966), Active wrench faults of Iran, Afghanistan and Pakistan, *Geol. Rundsch.*, *18*, 217–234.

Wessel, P., and W. H. F. Smith (1998), New, improved version of the Generic Mapping Tools released, *Eos Trans. AGU*, *79*(47), 579. [version 3.1]

Westaway, R. (1994), Present-day kinematics of the Middle East and eastern Mediterranean, *J. Geophys. Res.*, *99*, 12,071–12,090.

J. Jackson and R. Walker, Bullard Laboratories, Department of Earth Sciences, University of Cambridge, Madingly Road, Cambridge CB3 0EZ, UK. (jackson@esc.cam.ac.uk; rwalker@esc.cam.ac.uk)